SANDIA REPORT
SAND2017-13224
Unlimited Release
December 2017

Investigation of Energy Dissipation Behavior in Threaded Joints Under Impact Loading Using a Kolsky Tension Bar

Brett Sanborn and Bo Song
Sandia National Laboratories

Prepared by
Sandia National Laboratories
Albuquerque, New Mexico 87185 and Livermore, California 94550

Sandia National Laboratories is a multimission laboratory managed and operated by National Technology and Engineering Solutions of Sandia, LLC, a wholly owned subsidiary of Honeywell International, Inc., for the U.S. Department of Energy's National Nuclear Security Administration under contract DE-NA0003525.

Issued by Sandia National Laboratories, operated for the United States Department of Energy by National Technology and Engineering Solutions of Sandia, LLC.

Available to DOE and DOE contractors from
U.S. Department of Energy
Office of Scientific and Technical Information
P.O. Box 62
Oak Ridge, TN 37831

Telephone: (865) 576-8401
Facsimile: (865) 576-5728
E-Mail: reports@osti.gov
Online ordering: http://www.osti.gov/scitech

Available to the public from
U.S. Department of Commerce
National Technical Information Service
5301 Shawnee Rd
Alexandria, VA 22312

Telephone: (800) 553-6847
Facsimile: (703) 605-6900
E-Mail: orders@ntis.gov
Online order: https://classic.ntis.gov/help/order-methods/

SAND2017-13224
December 2017
Unlimited Release

Investigation of Energy Dissipation Behavior in Threaded Joints Under Impact Loading Using a Kolsky Tension Bar

Brett Sanborn, Bo Song
Experimental Environmental Simulation Department

Sandia National Laboratories
P. O. Box 5800
Albuquerque, New Mexico 87185-MS0557

Abstract

Threaded joints are a common fastening method in applications where disassembly may be required. With a fair amount of investigation of static behavior of threaded joints, less emphasis has been placed on the behavior of threaded joints subjected to transient impact loads. Understanding how energy is transferred across threaded joints under impact loading conditions is critical for improved design and optimization for extreme mechanical environments. Many factors, such as pre-torque, pre-tension load, and impact speed can affect how energy is transferred or dissipated across threaded joins. In addition, high-fidelity numerical simulation of mechanical response of threaded components under blast or impact loading requires reliable experiments and subsequent analyses. In this study, the energy dissipation behavior through a threaded joint under impact loading conditions is investigated using a Kolsky tension bar. The aim is to study possible energy dissipation behavior in both time and frequency domains while the threaded joint remains intact. New analytical methods to understand both time- and frequency-domain behavior of threaded joints are presented. Energy dissipation characteristics through steel-to-steel and steel-to-aluminum threaded joints were then investigated with varying parameters such as pre-torque and impact velocity.

ACKNOWLEDGMENTS

The authors would like to acknowledge Dennis Kenney, Thomas Martinez, and Randy Everett for their help conducting experiments.

The authors would also like to acknowledge the support of the TCG-XI community throughout the course of this project. Without the interest and support of the community, this project would not have been possible. Additionally, the support provided by the current and former Sandia JMP Program Managers, Sandia TCG-XI Leads, and Department Managers is gratefully acknowledged.

Sandia National Laboratories is a multimission laboratory managed and operated by National Technology and Engineering Solutions of Sandia, LLC., a wholly owned subsidiary of Honeywell International, Inc., for the U.S. Department of Energy's National Nuclear Security Administration under contract DE-NA-0003525.

TABLE OF CONTENTS

FIGURES

TABLES

1. INTRODUCTION

Threaded joints are a commonly used method for fastening components and assemblies in mechanical systems. Depending on the application, threaded joints may be subjected to impact loading conditions. Knowledge of the energy dissipation or transfer across a threaded joint while the joint remains intact, rather than failure, can aid in future improved designs and optimization of mechanical systems that experience impact loading. The total amount of energy dissipated through a threaded joint during a shock/impact event is analyzed within the time domain as a common practice. However, if energy dissipation is analyzed within the frequency domain, more information in terms of frequency-dependent energy dissipation may be provided for more efficient and effective design and optimization of threaded joints for protecting internal electrical or mechanical components in the system.

Very limited studies on impact energy transfer or dissipation through threaded joints are available in the literature and primarily focus on percussive drill rods in deep drilling of rocks [1]. In such configurations, several drill rods are threaded together and are subjected to both dynamic compression as well as torsional loading when drilling through rocks. When the percussive drill rods are subjected to impact, the joint typically remains within the elastic regime. Therefore, in such percussive drill rod studies, a Kolsky compression bar was used to transmit a compressive wave to a threaded joint and energy analyses in the time domain are performed on the basis of measured incident, reflected, and transmitted waves. Beccu and Lundberg [1] examined transfer of stress waves across threaded joints under different loading conditions in compression. For circumstances where the threaded joints are subjected to shock wave loading, a two-stage gas gun has been employed to characterize the threaded joints, where plastic deformation was identified to be the primary mechanism for energy dissipation [2].

Many factors can affect how threaded joint connections transfer energy. Related factors such as thread lubrication (dry/lubricated), bolt pre-tension, and pre-torque can all play a role in energy transfer across the threaded joint. In addition, impact speed may be another significant factor which can affect impact energy transfer/dissipation. Therefore, it is desirable to establish a reliable experimental procedure from specimen design, experiment design and execution, and data analysis to systematically investigate the characteristics of impact energy transfer/dissipation through threaded joints under various conditions.

In this study, a Kolsky tension bar was used to investigate the energy transfer across threaded joints subjected to different impact speeds. The joint material type was varied (steel/steel and steel/aluminum) as well as the pre-torque on the different joints. Analytical methods in terms of energy dissipation ratio in both time and frequency domain are developed and applied to determine the energy dissipation through the steel/steel and steel/aluminum threaded joints.

This page intentionally left blank.

2. KOLSKY TENSION BAR FOR DYNAMIC THREADED JOINT INVESTIGATION

In this section, the experimental techniques used to study the behavior of threaded joints under impact loading are presented.

2.1. Dynamic Characterization of Threaded Joints Using a Kolsky Tension Bar

To investigate energy dissipation behavior across threaded joint interfaces, a Kolsky tension bar as shown in Fig. 1 was used. This apparatus has also been previously presented in detail [3]. In the Kolsky tension bar shown in Fig. 1, the striker is contained inside a gun barrel and is launched using compressed gas. When the striker impacts the end cap on the end of the gun barrel, a tension pulse is generated and then propagates along the gun barrel and transmits into the incident bar through a coupler. To minimize interfaces and to ensure that the pulse is transferred from the incident bar to the transmission bar only across the threaded joint interface under investigation, a transmission bar with male ½ inch-20 threads was machined to thread into the female incident bar, as shown in Fig. 2. In this study, the incident bar was 12 feet long while the transmission bar was 7 feet long. Both the incident and transmission bars were made of C300 maraging steel to create a steel/steel threaded joint. A 6061-T6 aluminum transmission bar was also selected to investigate a steel/aluminum threaded joint. All bars were 1-inch diameter.

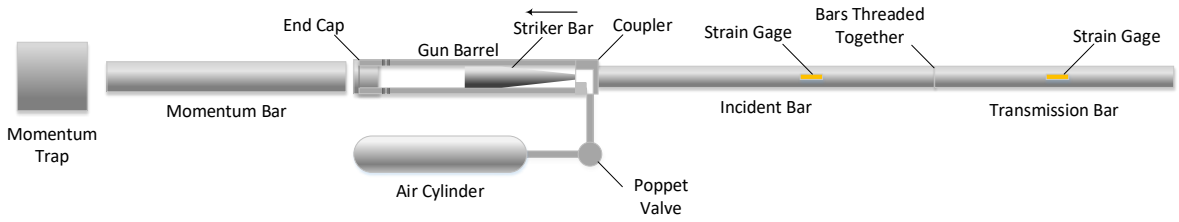

Figure 1. Kolsky Bar setup used to measure energy transfer across threaded joints in tension

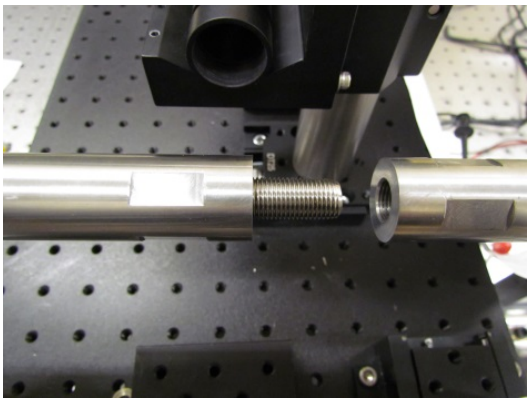

Figure 2. Kolsky Bar ends

The interest of current study is the impact energy dissipation through a threaded joint not only in the time domain but also in the frequency domain. It is desirable to generate and transfer a pulse with a wide frequency range from the incident bar to the threaded joint. To accomplish this goal, a tapered striker as shown in Fig. 3 was designed. The striker used in this study was different in a couple of ways compared to the strikers typically used in Kolsky bar experiments. First, the striker was made of tungsten. A tungsten striker impacting on a steel incident bar produces a pulse with a short rise time and a stepwise decreasing unloading tail due to the higher mechanical impedance of the tungsten striker than that of the incident bar [4]. Second, to achieve a relatively smooth unloading tail, the rear two-thirds of the striker was tapered. A comparison of the generated strain pulses using a typical cylindrical steel striker and the tapered tungsten striker is shown in Fig. 4. No pulse shaping material was used in this case so as not to limit the rise time of the incident pulse. As shown in Fig 4, both strikers produced similarly fast rise times of approximately 40 μs. However, the cylindrical steel striker produced a typical square pulse that is expected from coaxial impact of two rods with matching impedance. The tapered tungsten striker has a longer unloading tail that is relatively smooth compared to the stepwise unloading tail that would be generated by a cylindrical striker made of tungsten. This expands the total frequency content of the pulse, as is shown in Fig. 5. The cylindrical steel striker was not able to generate the frequency content at and above 15 kHz. However, when a tapered tungsten striker was used, this frequency limit extends from 15 kHz to 23 kHz, even though the tapered tungsten striker was longer than the cylindrical steel striker. Utilizing a wider frequency range provides better understanding of the behavior of threaded joints at higher frequencies.

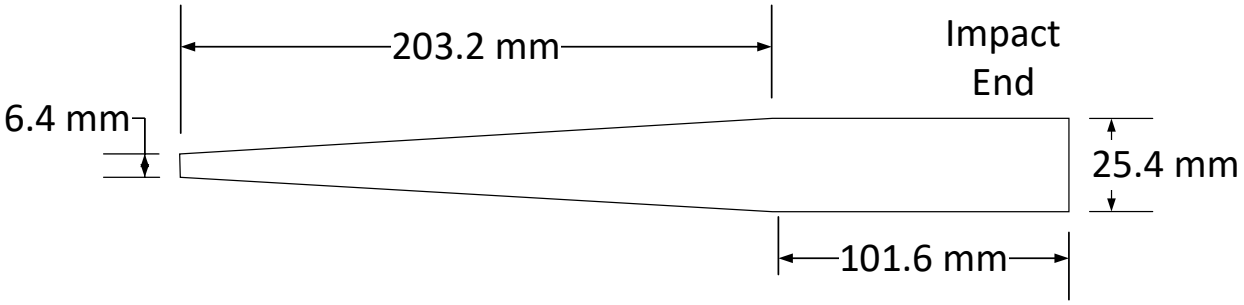

Figure 3. Detailed design of the tapered tungsten striker used in this study

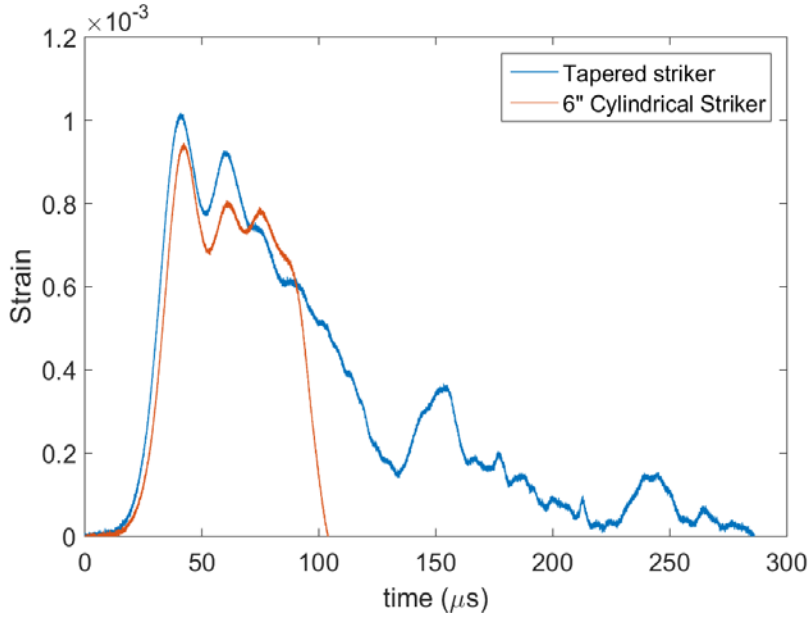

Figure 4. Time history comparison of the tapered tungsten striker and a cylindrical steel striker impacting a steel incident bar

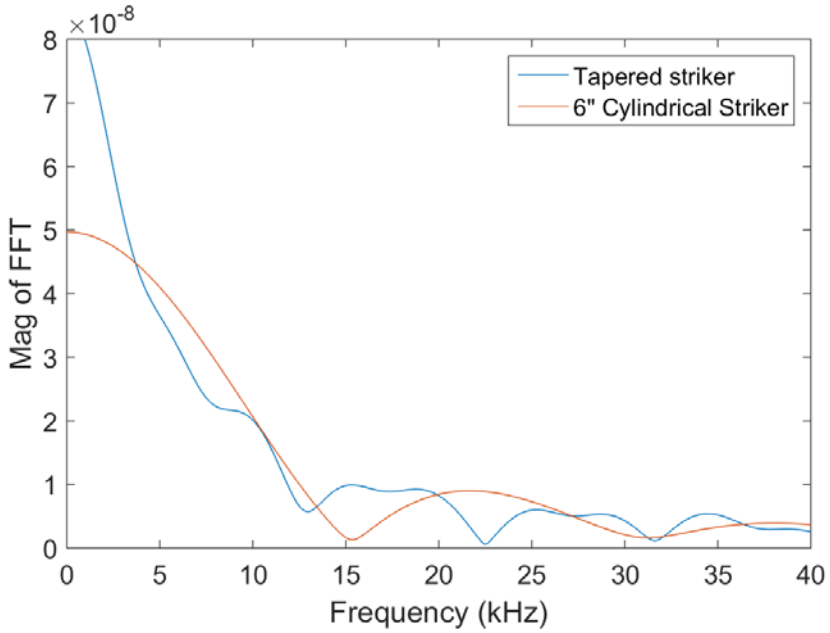

Figure 5. Comparison of frequency content using the tapered tungsten striker and a cylindrical steel striker impacting a steel incident bar

2.2. Energy Analysis in the Time Domain

There is limited knowledge and methodology to analyze the energy associated with Kolsky bar experiments. Beccu and Lundberg [1] provided the energies associated with bar strains measured in a Kolsky bar experiment to analyze the energy transfer through threaded joints. Lok et al. [5] also provided the same formula to calculate the time history of energy in Kolsky bar experiments. For a measured strain, $\varepsilon(t)$, within a bar, the energy, E, was calculated with [1]

$$\mathrm{E} = E_0 C_0 A_0 \int_0^t \varepsilon(t)^2 dt \tag{1}$$

where E_0, C_0, and A_0 are Young's modulus, elastic wave speed, and cross-sectional area of the pressure bar. When a constant strain, like a square pulse generated in a conventional Kolsky compression bar experiment, is generated within a bar, Equation (1) becomes

$$\mathrm{E} = E_0 C_0 A_0 \varepsilon^2 T \tag{2}$$

where T is the total duration of loading. Equation (2) is consistent with the calculation by Song and Chen [6]. Compared to the analysis in Ref. [1], Song and Chen [6] described that the energy associated with a bar strain consists of two parts, kinetic and strain energies, equally.

For an arbitrary bar strain, the associated kinetic energy per unit bar length is calculated as

$$dE_k(t) = \frac{1}{2}V(t)^2\,dm = \frac{1}{2}\rho_0 A_0 V(t)^2\,dl = \frac{1}{2}\rho_0 A_0 V(t)^2 C_0\,dt \tag{3}$$

According to one-dimensional stress wave propagation theory, we have

$$V(t) = C_0\varepsilon(t) \tag{4}$$

Applying Equation (4) into Equation (3) yields

$$dE_k(t) = \frac{1}{2}\rho_0 A_0 C_0^3 \varepsilon(t)^2\,dt \tag{5}$$

For an elastic stress wave, $E_0 = \rho_0 C_0^2$, then Equation (5) can be rewritten as

$$dE_k(t) = \frac{1}{2}E_0 C_0 A_0 \varepsilon(t)^2\,dt \tag{6}$$

Similarly, the strain energy per unit bar length is calculated as

$$dE_s(t) = \int_0^{\varepsilon(t)} \sigma d\varepsilon \cdot dV = \int_0^{\varepsilon(t)} E_0 \varepsilon d\varepsilon \cdot A_0 dl = \frac{1}{2}E_0 C_0 A_0 \varepsilon(t)^2\,dt \tag{7}$$

Therefore, the kinetic and strain energies are equal and the total energy is

$$dE(t) = dE_k(t) + dE_s(t) = E_0 C_0 A_0 \varepsilon(t)^2\,dt \tag{8}$$

The total energy over a certain amount of time is thus calculated with integral of Equation (8),

$$E(t) = E_0 C_0 A_0 \int_0^t \varepsilon(t)^2\,dt \tag{9}$$

Equation (9) has exactly the same form as provided by Beccu and Lundberg [1]. However, the detailed derivation is provided in this study.

In a Kolsky bar experiment, the impact of the striker on the incident bar end generates a stress wave that propagates down the incident bar. The incident stress wave is partially reflected back as a reflected pulse and is partially transmitted into the transmission bar while the specimen is deformed. The incident stress wave can be of any shape due to pulse shaping. Regardless of the profiles, the energies associated with the incident, reflected, and transmitted pulses are expressed with Equation (9) as

$$E_i(t) = E_0 C_0 A_0 \int_0^t \varepsilon_i(t)^2\,dt \tag{10a}$$

$$E_r(t) = E_0 C_0 A_0 \int_0^t \varepsilon_r(t)^2 dt \tag{10b}$$

$$E_t(t) = E_1 C_1 A_1 \int_0^t \varepsilon_t(t)^2 dt \tag{10c}$$

where the subscripts, *i*, *r*, and *t* represent the incident, reflected, and transmitted pulses, respectively. Here, E_0, C_0, and A_0 are Young's modulus, elastic wave speed, and cross-sectional area of the incident bar, respectively; whereas, E_1, C_1, and A_1 are Young's modulus, elastic wave speed, and cross-sectional area of the transmission bar, respectively. The input and output energies of the specimen are then expressed as

$$E_{input}(t) = E_i(t) - E_r(t) = E_0 C_0 A_0 \int_0^t \left[\varepsilon_i(t)^2 - \varepsilon_r(t)^2\right] dt \tag{11}$$

$$E_{output}(t) = E_t(t) = E_1 C_1 A_1 \int_0^t \varepsilon_t(t)^2 dt \tag{12}$$

The energy dissipated in the specimen is

$$\Delta E(t) = E_{input}(t) - E_{output}(t) = E_0 C_0 A_0 \int_0^t \left[\varepsilon_i(t)^2 - \varepsilon_r(t)^2\right] dt - E_1 C_1 A_1 \int_0^t \varepsilon_t(t)^2 dt \tag{13}$$

The energy dissipation (Equation (13)) can also be derived and understood in a different way. In a typical Kolsky compression bar experiment, the incident bar pushes the specimen and then the specimen pushes the transmission bar in the same direction but at a lower speed. This process can be understood that the incident bar applies work to the specimen and the specimen then releases a portion of the work back to the transmission bar. The work that the incident bar applies to the specimen can be calculated as

$$dW_i(t) = F_i(t) dL_i \tag{14}$$

where

$$F_i(t) = E_0 A_0 \left[\varepsilon_i(t) + \varepsilon_r(t)\right] \tag{15}$$

$$dL_i = V_i(t) dt = C_0 \left[\varepsilon_i(t) - \varepsilon_r(t)\right] dt \tag{16}$$

Equation (14) is then rewritten as

$$dW_i(t) = E_0 C_0 A_0 \left[\varepsilon_i(t)^2 - \varepsilon_r(t)^2\right] dt \tag{17}$$

Therefore, the total work that the incident bar applies to the specimen is

$$W_{input}(t) = E_0 C_0 A_0 \int_0^t \left[\varepsilon_i(t)^2 - \varepsilon_r(t)^2\right] dt \tag{18}$$

This derivation has the same form as Equation (11). The work that the specimen (in this case, threads) applies to the transmission bar is,

$$dW_{output}(t) = F_t(t) dL_t \tag{19}$$

where

$$F_t = E_1 A_1 \varepsilon_t(t) \tag{20}$$

$$dL_t = V_t(t) dt = C_1 \varepsilon_t(t) dt \tag{21}$$

Equation (19) then becomes

$$dW_{output}(t) = E_1 C_1 A_1 \varepsilon_t(t)^2 dt \tag{22}$$

The work that the specimen releases back to the transmission bar has the same form as Equation (12),

$$W_{output}(t) = E_1 C_1 A_1 \int_0^t \varepsilon_t(t)^2 dt \tag{23}$$

The net work that is applied to the specimen is

$$\Delta W(t) = W_{input}(t) - W_{output}(t) = E_0 C_0 A_0 \int_0^t \left[\varepsilon_i(t)^2 - \varepsilon_r(t)^2\right] dt - E_1 C_1 A_1 \int_0^t \varepsilon_t(t)^2 dt \tag{24}$$

This work correlates to the energy that is expressed with Equation (13) and dissipates in the specimen.

The energy dissipation ratio is then calculated as

$$\delta(t) = \frac{\Delta E(t)}{E_{input}(t)} = 1 - \frac{E_1 C_1 A_1}{E_0 C_0 A_0} \cdot \frac{\int_0^t \varepsilon_t(t)^2 dt}{\int_0^t \left[\varepsilon_i(t)^2 - \varepsilon_r(t)^2\right] dt} \tag{25}$$

When the incident and transmission bars are made of the same material and have the same cross-sectional area, Equations (13) and (25) are simplified as

$$\Delta E(t) = E_{input}(t) - E_{output}(t) = E_0 C_0 A_0 \int_0^t \left[\varepsilon_i(t)^2 - \varepsilon_r(t)^2 - \varepsilon_t(t)^2\right] dt \tag{26}$$

$$\delta(t)=\frac{\Delta E(t)}{E_{input}(t)}=1-\frac{\int_0^t \varepsilon_t(t)^2\,dt}{\int_0^t\left[\varepsilon_i(t)^2-\varepsilon_r(t)^2\right]dt} \tag{27}$$

Equation (26) is consistent with the analysis by Lok et al. [5].

2.3. Energy Analysis in the Frequency Domain

Just as in typical Kolsky bar tests for material property characterization, the strain gage signals collected from the incident and transmission bars are used to probe the frequency-domain energy dissipation behavior of the threaded joints.

A strain signal, $\varepsilon(t)$, can be expressed in the frequency domain with a Fourier transform,

$$\varepsilon(f)=\int_{-\infty}^{+\infty}\varepsilon(t)\cdot e^{-i2\pi ft}dt=B(f)e^{-i(2\pi f+\phi)} \tag{28}$$

where B and ϕ are magnitude and phase of the Fourier transform, respectively; f is frequency. According to Fourier transform principles, the energy spectral density is expressed as

$$S(f)=A_0C_0E_0|B(f)|^2 \tag{29}$$

The energy spectral density represents the energy distribution over frequencies or the energy per unit frequency. Therefore, the energy at a specific frequency is calculated as

$$E(f)=\int_f^{f+\Delta f}S(f)df=A_0C_0E_0\int_f^{f+\Delta f}|B(f)|^2df\approx A_0C_0E_0|B(f)|^2\Delta f \tag{30}$$

The energies associated with the incident, reflected, and transmitted strains can be expressed in the frequency domain as the follows,

$$E_i(f)=A_0C_0E_0|B_i(f)|^2\Delta f \tag{31a}$$

$$E_r(f)=A_0C_0E_0|B_r(f)|^2\Delta f \tag{31b}$$

$$E_t(f)=A_1C_1E_1|B_t(f)|^2\Delta f \tag{31c}$$

where $B_i(f)$, $B_r(f)$, and $B_t(f)$ are the magnitudes of Fourier transforms on the incident, reflected, and transmitted strains, respectively. Like the analysis in the time domain, the total input and output energies through the specimen can be expressed in the frequency domain,

$$E_{input}(f) = E_i(f) - E_r(f) = A_0 C_0 E_0 \left[|B_i(f)|^2 - |B_r(f)|^2 \right] \Delta f \tag{32}$$

$$E_{output}(f) = E_t(f) = A_1 C_1 E_1 |B_t(f)|^2 \Delta f \tag{33}$$

The energy dissipated in the specimen is

$$\Delta E(f) = E_{input}(f) - E_{output}(f) = \left\{ A_0 C_0 E_0 \left[|B_i(f)|^2 - |B_r(f)|^2 \right] - A_1 C_1 E_1 |B_t(f)|^2 \right\} \Delta f \tag{34}$$

The frequency-based energy dissipation ratio is calculated as

$$\delta(f) = \frac{\Delta E(f)}{E_{input}(f)} = 1 - \frac{A_1 C_1 E_1}{A_0 C_0 E_0} \cdot \frac{|B_t(f)|^2}{|B_i(f)|^2 - |B_r(f)|^2} \tag{35}$$

when the incident and transmission bars are made of the same material and have the same cross-sectional area, Equations (34) and (35) are re-written as

$$\Delta E(f) = E_{input}(f) - E_{output}(f) = A_0 C_0 E_0 \left[|B_i(f)|^2 - |B_r(f)|^2 - |B_t(f)|^2 \right] \Delta f \tag{36}$$

$$\delta(f) = \frac{\Delta E(f)}{E_{input}(f)} = 1 - \frac{|B_t(f)|^2}{|B_i(f)|^2 - |B_r(f)|^2} \tag{37}$$

As described above, the impact energy dissipation can be calculated in either time or frequency domain. However, when a stress wave propagates through a threaded joint, it can be significantly disturbed due to multiple interfaces at threads. Each interface may generate a small reflection of the stress wave back to the incident bar. In fact, the measured reflected pulse is a consequence of stress wave reflection at multiple interfaces. Uncertainties thus exist in the time-stamped reflected pulse and transfer to the time history of impact energy dissipation calculated with Equations (26) and (27). However, the total amount of energy dissipated over the entire duration of loading may still be reliable. Compared to the time-domain analysis, the energy dissipation in the frequency domain is more reliable as the energy calculated at each frequency has accounted for the entire duration of loading.

This page intentionally left blank.

3. DYNAMIC EXPERIMENTS ON THREADED JOINTS

This section summarizes the experimental test plan for steel/steel and steel/aluminum threaded joints as well as the data processing procedure.

3.1. Experimental Matrix

As mentioned earlier, many factors can influence how energy is transferred across a threaded joint. In this study, the effects of pre-torque on the joint, impact velocity, and material type were investigated. Table 1 shows the experimental matrix for a steel incident bar and a steel transmission bar (steel/steel threaded joint). Note that the transmission bar was machined with male threads while the incident bar had female threads. There is only one interface which is the threaded joint between the strain gages on the incident and transmission bars such that the energy dissipation calculated with the strain gage signals (Equations (26) and (27)) is specified to the threaded joints. As shown in Table 1, the steel/steel threaded joint was subjected to two torque levels of "hand-tight", which had minimal torque, and 50 ft-lbs of torque. The actual amplitude of preload generated in the pre-torqued threaded joints is notoriously variable despite using calibrated torque wrenches and has shown to vary +/- 35% [7]. Adding lubrication only improves the pre-tension variability to approximately +/- 25%. The variability has also been reduced by using "instrumented bolts" which have integrated strain gages [8]. These variations may even generate more significant variation in impact energy transfer/dissipation characteristics. The impact velocities were 4, 9.6, and 13.5 m/s and five experiments were repeated at each velocity.

Table 1. Experimental plan for C300 steel/C300 steel threaded joint

Material	**Torque (ft-lb)**	**4 m/s (# experiments)**	**9.6 m/s (# experiments)**	**13.5 m/s (# experiments)**
Steel/Steel	"hand-tight"	5	5	5
Steel/Steel	50	5	5	5

The test matrix for steel/aluminum threaded joints are shown in Table 2. Different velocities and torques were chosen for the steel/aluminum threaded joint experiments because the aluminum has a lower yield strength than the maraging steel and could easily become yielded or even fractured if the striker velocity was too high. Similarly, the pre-set torque was lower to prevent over-torqueing and possible plastic deformation in the threads.

Table 2. Experimental plan for C300 steel/6061-T6 aluminum threaded joint

Material	**Torque (ft-lb)**	**1.7 m/s (# experiments)**	**3.7 m/s (# experiments)**	**6 m/s (# experiments)**
Steel/Aluminum	"hand-tight"	5	5	5
Steel/Aluminum	17	5	5	5

3.2. Dynamic Experimental Procedure

Figure 6 shows a typical original record of an experiment on a steel/steel threaded joint. As shown in Fig. 6., the transmitted pulse is nearly the same in amplitude as the incident pulse, meaning most of the impact energy was transmitted across the threaded joint. The individual incident, reflected, and transmitted strain time-histories are shown in Fig. 7. Using Equation (10), the total energy associated with each signal was calculated in the time domain and is shown in Fig. 8. Finally, the energy loss as a function of time was calculated using Equation (26) and is shown in Fig. 9. As shown in Fig. 9, the energy loss increases during loading, due to elastic deformation of the threads, and then decreases after unloading starts, and gets back to zero when the dynamic test is completed. This means that when the threaded joint is subjected to dynamic loading, the threaded joint absorbs dynamic impact energy for elastic deformation and then releases the elastic deformation energy back to the bar system during unloading until fully recovered.

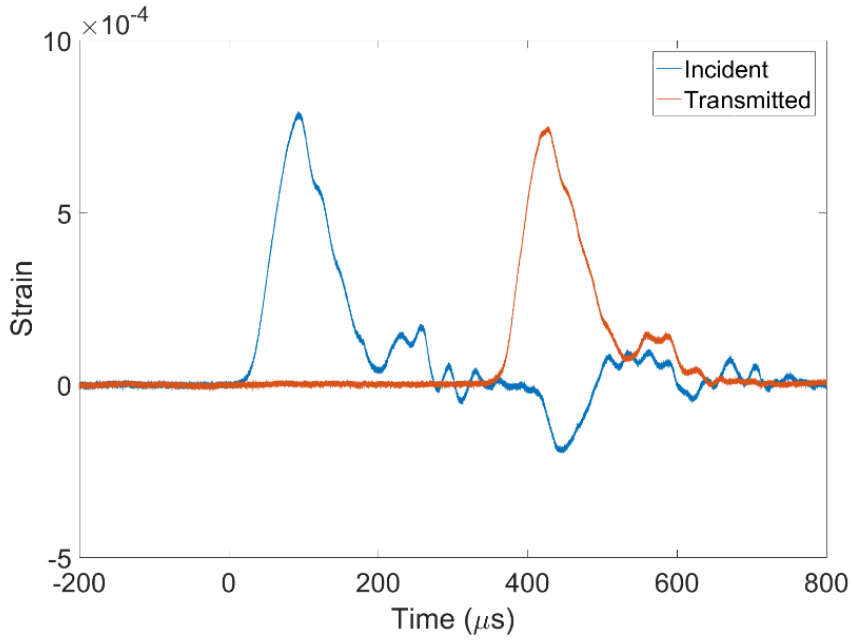

Figure 6. Original experimental record of a steel/steel threaded joint

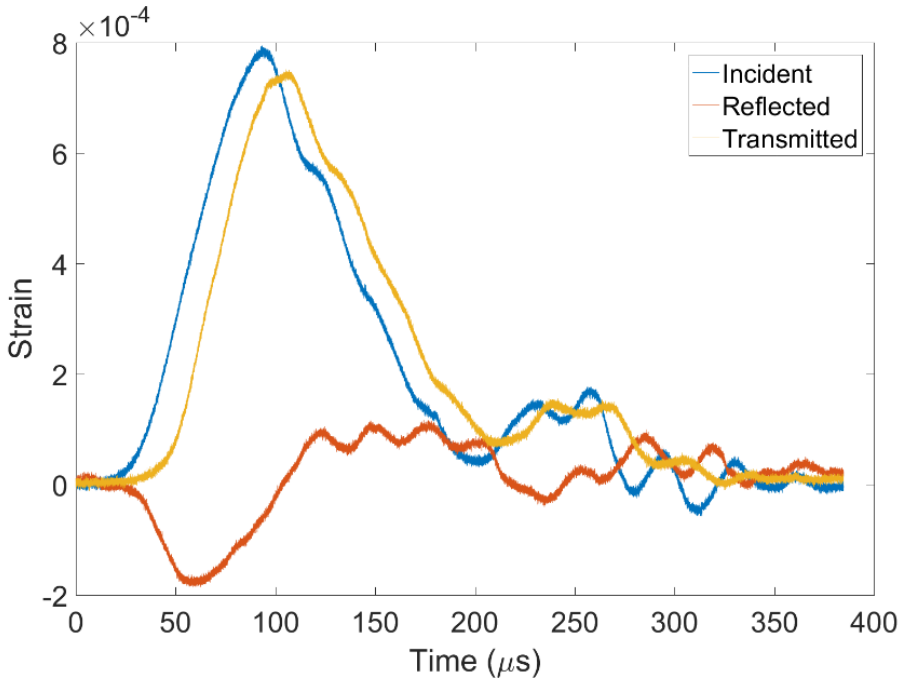

Figure 7. Time domain strain signals from an experiment on a steel/steel threaded joint

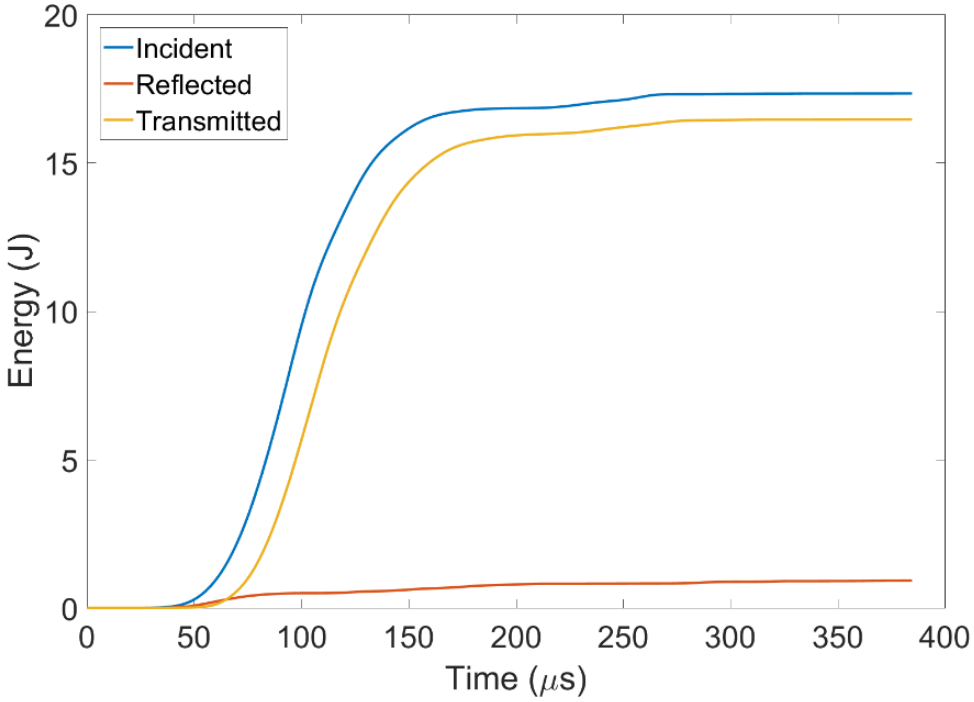

Figure 8. Energy of each signal in the time domain

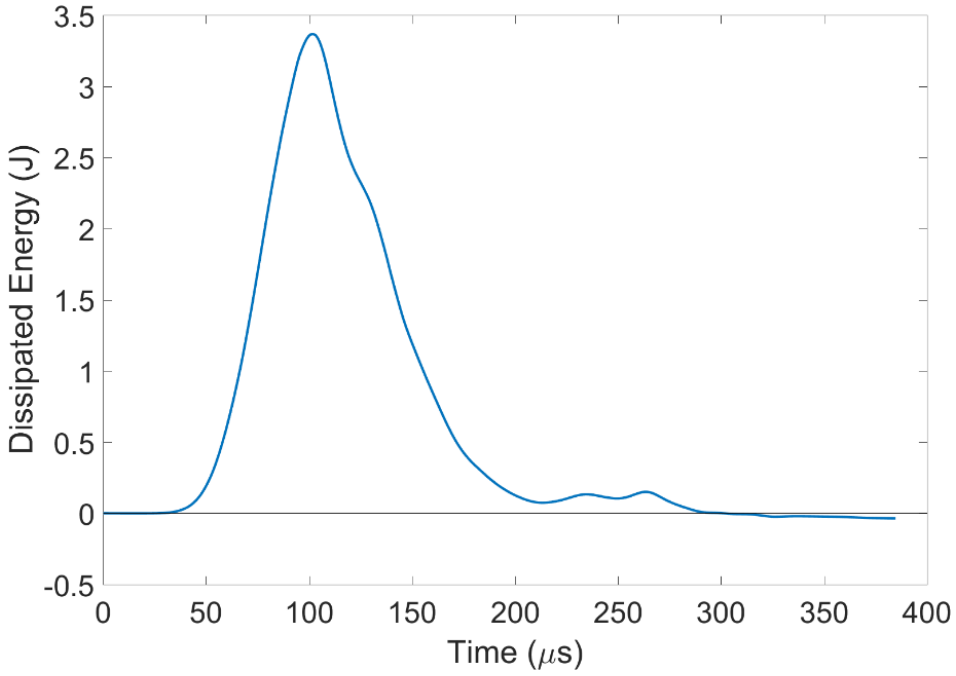

Figure 9. Dissipated energy as a function of time

The impact energy dissipation was also analyzed in the frequency domain. Using Equation (28), the magnitude of the strain signals is calculated and shown in Fig. 10. The strain signal FFTs are converted to energy spectrum densities (Equation (29)) and are shown in Fig. 11. The energy spectrum density in the frequency domain is interpreted as the energy distribution over different frequencies. The energy spectrum density of each signal is used with Equation (37) to obtain the energy dissipation ratio in the frequency domain and is shown in Fig 12. Investigating energy dissipation ratio in this way as a function of frequency is beneficial since the dissipation behavior of the threaded joint at specific frequencies can be known. As shown in Fig. 12, the energy dissipation ratio shows discontinuity at and above 10 kHz. This is because there was no or very small input impact energy at and above 10 kHz (Fig. 11). In addition, nearly no energy was dissipated for the frequencies below 2 kHz. The energy between 2-4 kHz was dissipated with a ratio of ~0.05. However, at the frequencies above 4 kHz, a negative energy dissipation is observed meaning energy gain. This indicates that the dissipated energy between 2-4 kHz might not be totally lost but were transferred to different frequencies above 4 kHz, which may be described as "frequency shift." Therefore, the impact energy was not nominally dissipated but internally shifted to different frequencies. This is consistent with the time-domain analysis (Fig. 9) where nearly no energy dissipation was observed after dynamic test. The comparison of the analyses in the time domain (Fig. 9) and the frequency domain (Fig. 12) shows that, even though there was no impact energy nominally dissipated in the time domain, the energy may still be dissipated at some frequencies and gained at other frequencies. This information also indicates that the frequency-domain analysis provides much more information than the time-domain analysis, which may be helpful for more effective design of threaded joint to protect frequency-sensitive devices or components.

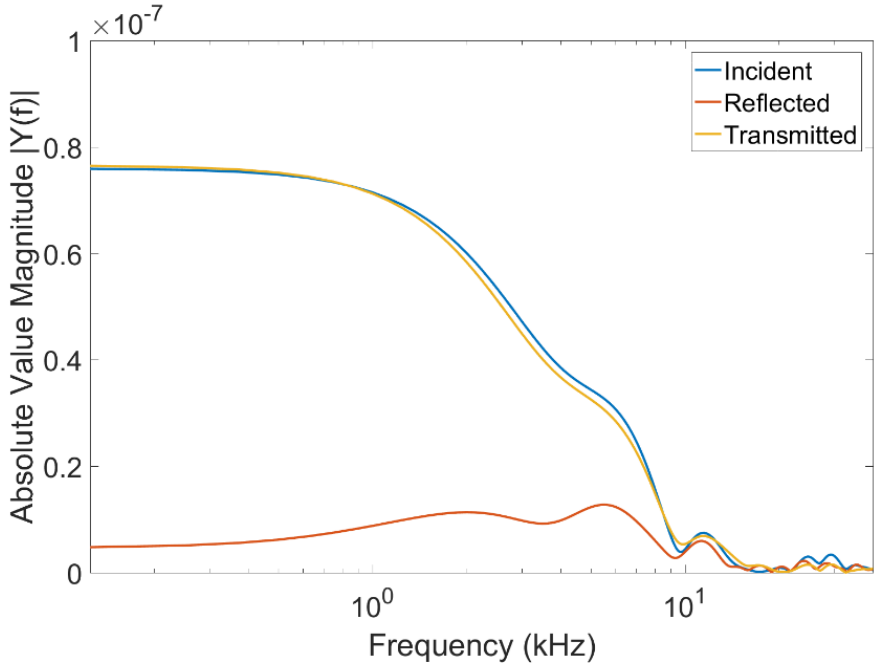

Figure 10. Strain signals converted to frequency domain

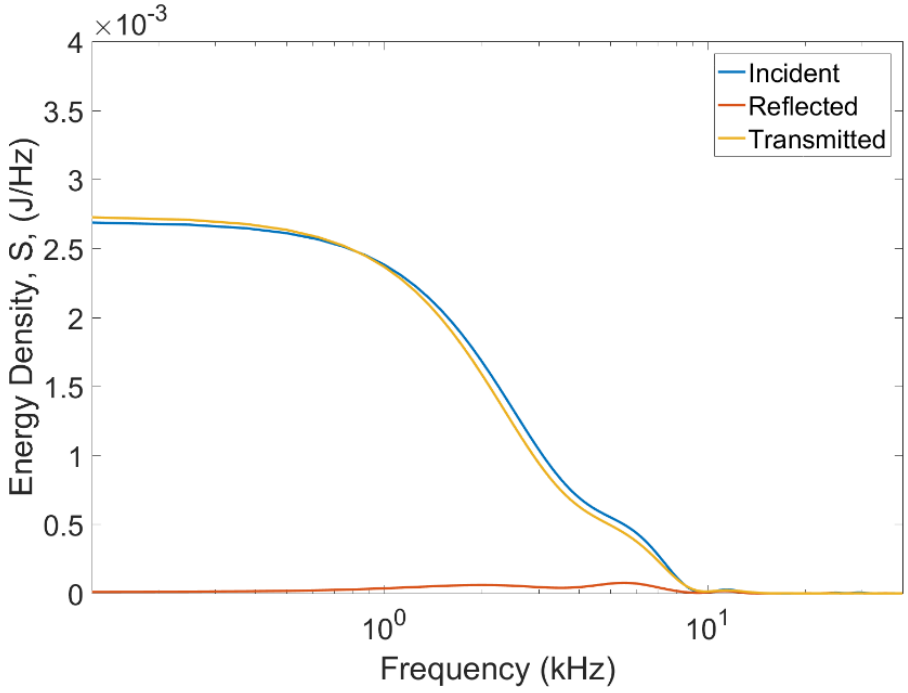

Figure 11. Energy spectrum densities of strain signals

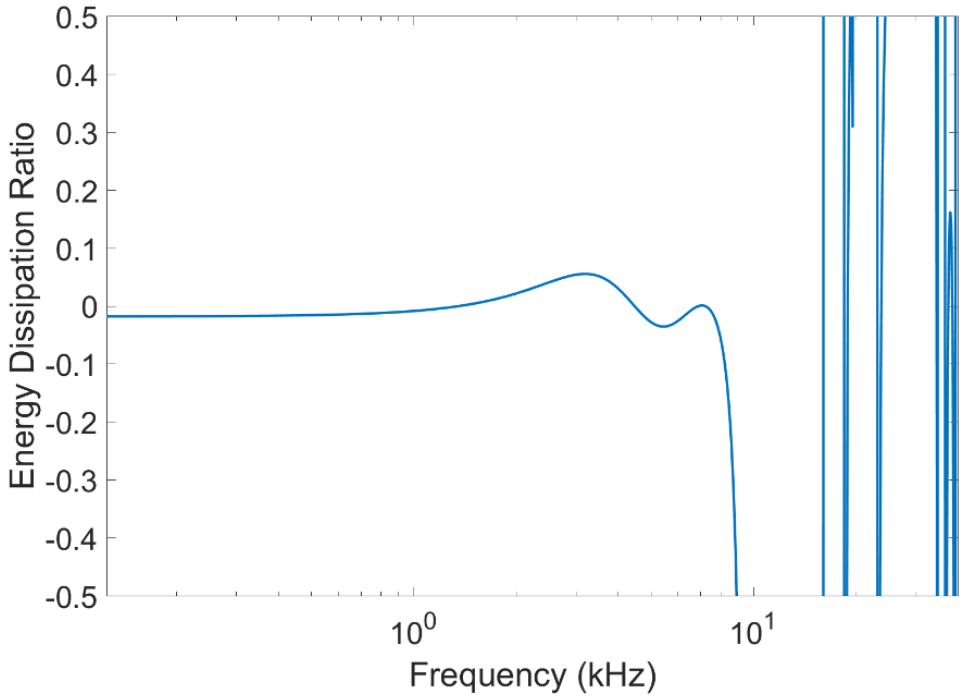

Figure 12. Energy dissipation ratio as a function of frequency for steel/steel threaded joint

4. EXPERIMENTAL RESULTS AND DISCUSSION

Following the same experimental procedure, the results from experimental matrices in Tables 1 and 2 are presented. The Kolsky experimental results are evaluated for repeatability in both the time and frequency domains.

4.1. Threaded Joint Experimental Results and Discussion

4.1.1. Steel/Aluminum Threaded Joint

The time histories of the incident, reflected, and transmitted pulses from experiments at hand-tight torque for steel/aluminum threaded joints are shown in Fig. 13. Legend entries are simply the experiment number. Good repeatability is seen for each of the impact velocities despite not using a specific torque setting or torque wrench. Experiments at the higher pre-torque setting and other impact velocities have similarly good repeatability.

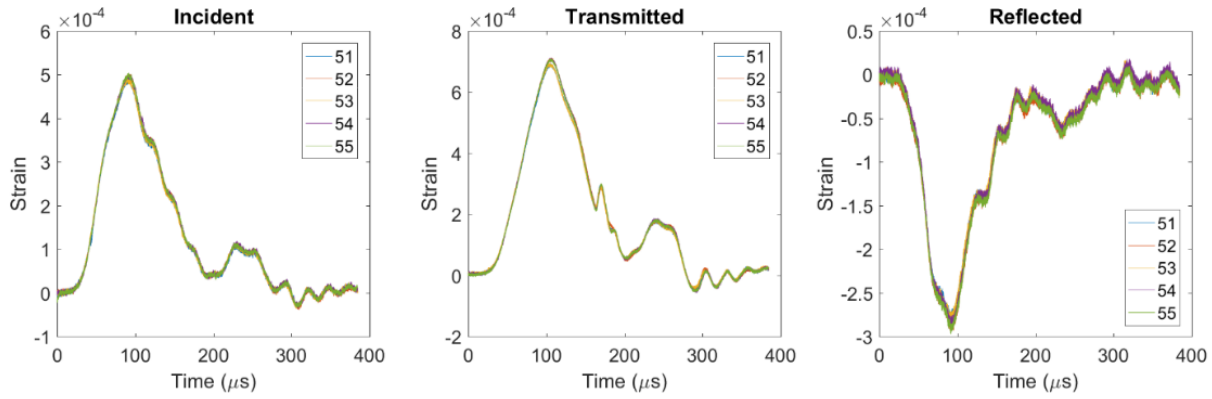

Figure 13. Time domain incident, reflected, and transmitted pulses for steel/aluminum joints at hand tight torque at 3.7 m/s impact velocity

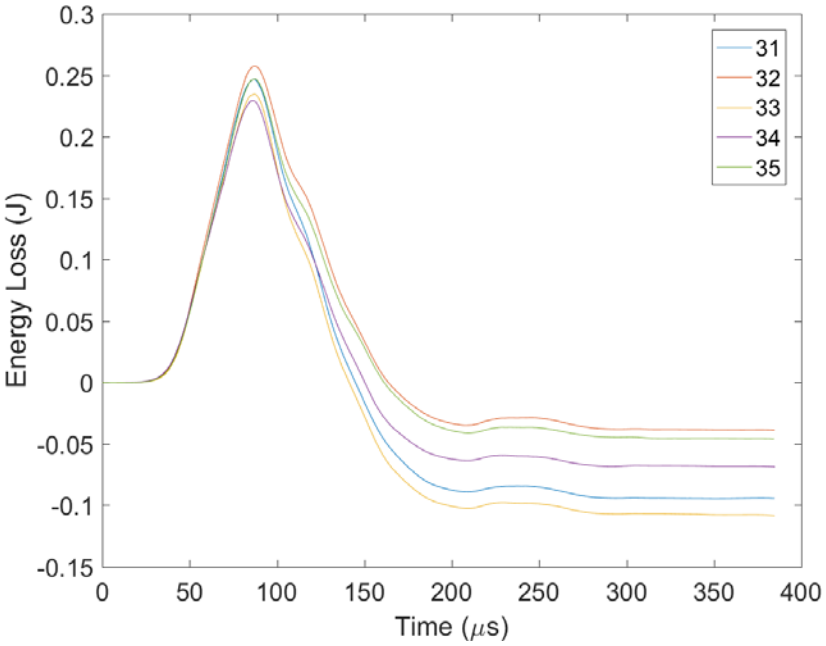
Energy Loss (J)
Time (μs)
31
32
33
34
35

(a)

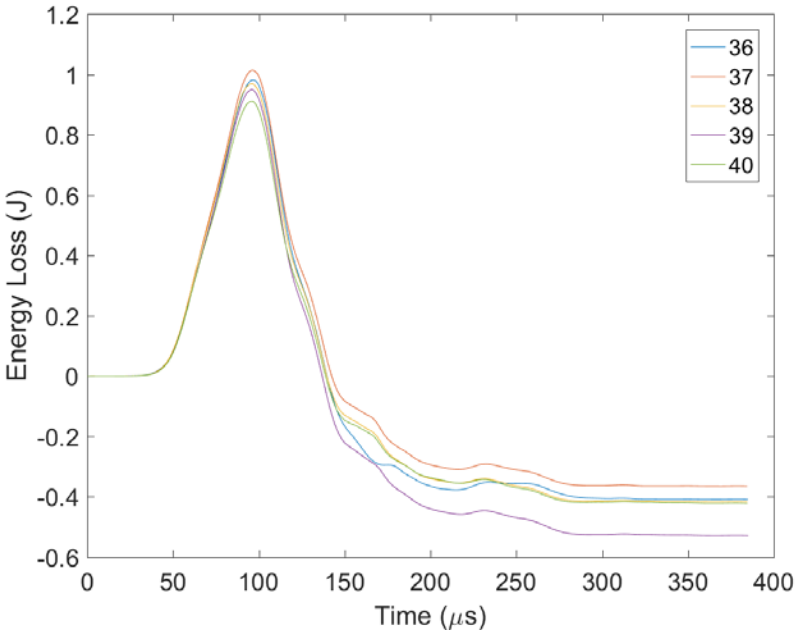
Energy Loss (J)
Time (μs)
36
37
38
39
40

(b)

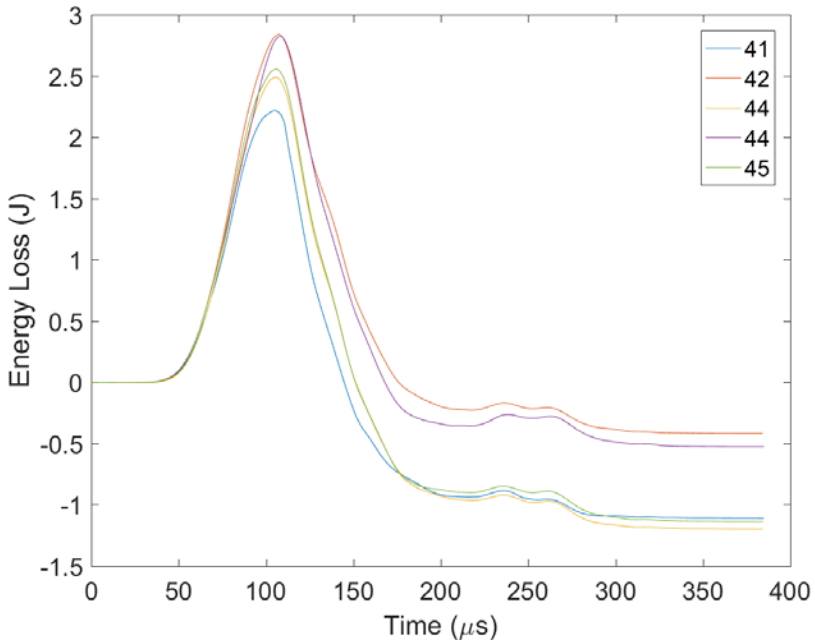

c)

Figure 14. Time-domain energy dissipation ratios for steel/aluminum threaded joints at hand-tight torque for a) 1.7 m/s, b) 3.7 m/s, c) 6 m/s impact velocity

Energy loss in the time domain for the steel/aluminum threaded joint calculated using Equation (13) is for hand-tight torque at three impact speeds is shown in Fig. 14. As Fig. 14 shows, energy is dissipated during the rise of the signal and peaks at different levels depending on the impact speed. After unloading begins at around 100 µs in each plot, the energy loss begins to decrease. The total energy loss drops below zero as the unloading continues past approximately 150 µs.

The frequency domain energy dissipation ratio is plotted for each experiment on steel/aluminum threaded joint under hand-tight torque in Fig. 15. The frequency domain energy dissipation behavior shows more variability compared to the time-domain strain pulses, but there are some commonalities mainly at the peak energy dissipation ratio around 6.5 kHz at 1.7 m/s impact speed. The dissipation ratios at 3.7 m/s show some difference between the first experiment (#36) compared to the remaining four experiments at that speed, namely a higher dissipation ratio at low frequencies that decreases with successive impacts, followed by an increase in peak dissipation ratio that occurs around 4-6 kHz, indicating that there might be some change in the threaded joint with each successive experiment. The energy dissipation behavior at 6 m/s impact speed is uniform except for the initial dissipation behavior at frequencies below 1 kHz, where the dissipation ratio varied from -0.15 to -0.01, while a peak is still present at 4.5 kHz.

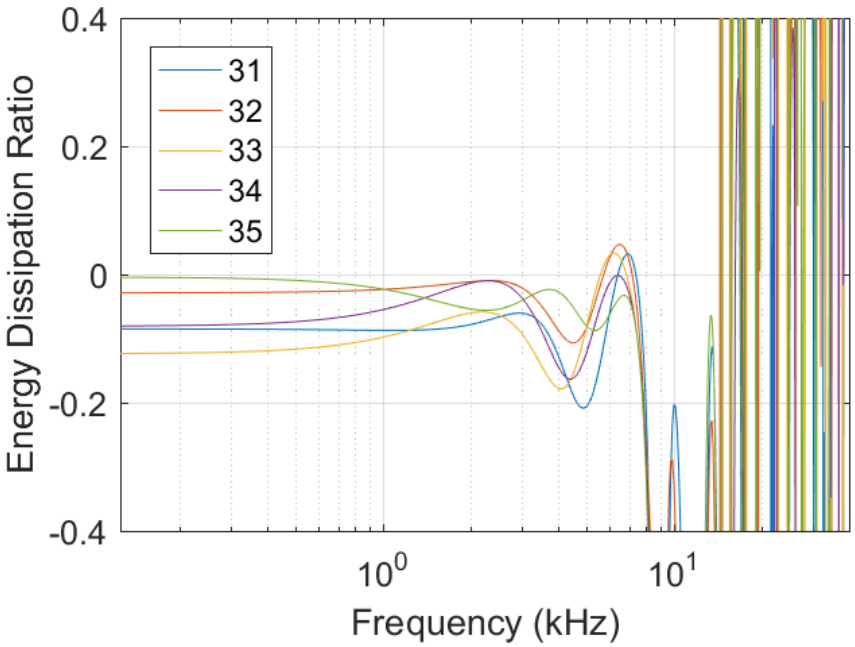
0.4
0.2
0
-0.2
-0.4
Energy Dissipation Ratio
31
32
33
34
35
10^0
10^1
Frequency (kHz)

(a)

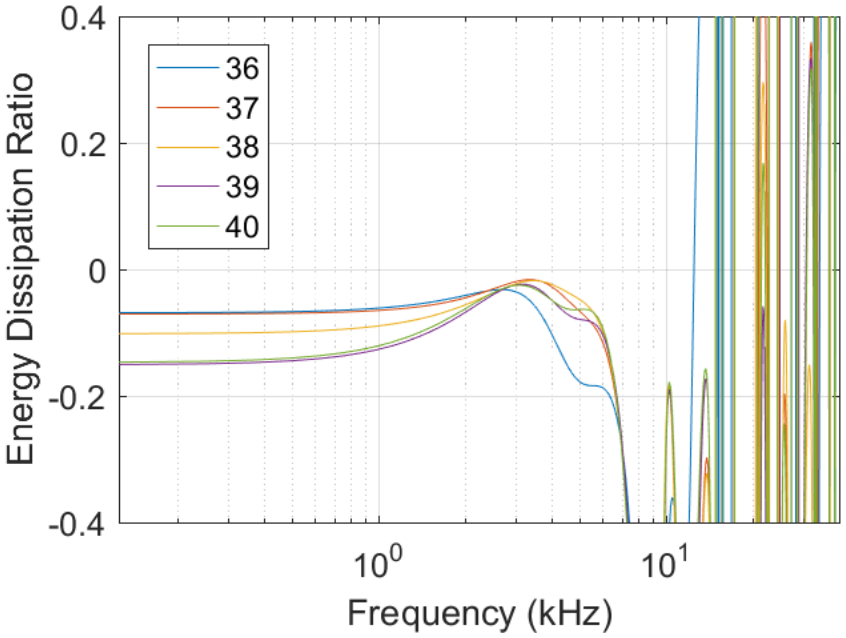
0.4
0.2
0
-0.2
-0.4
Energy Dissipation Ratio
36
37
38
39
40
10^0
10^1
Frequency (kHz)

(b)

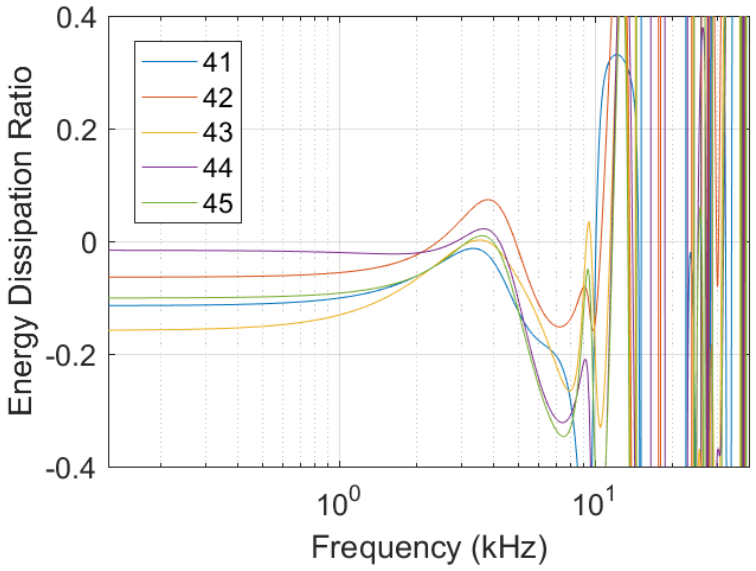

(c)

Figure 15. Frequency-domain energy dissipation ratios for steel/aluminum threaded joints at hand-tight torque for a) 1.7 m/s, b) 3.7 m/s, c) 6 m/s impact velocity

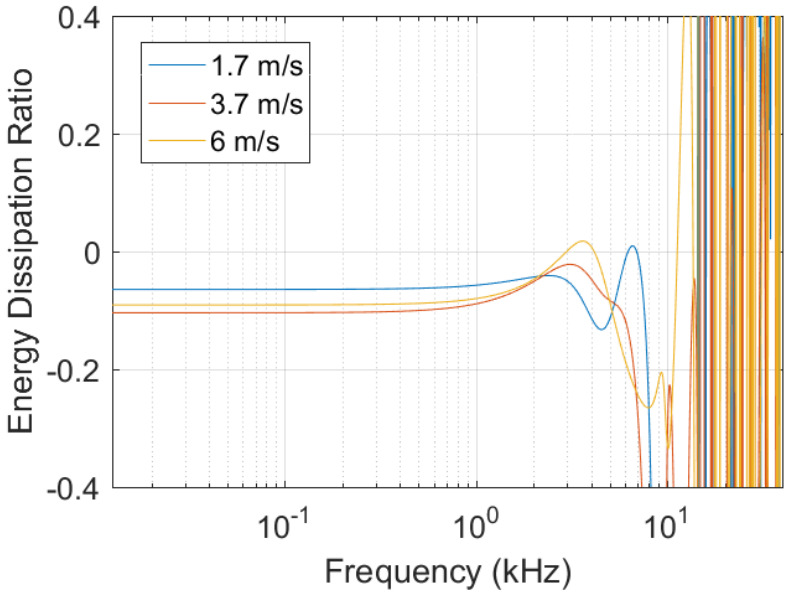

Figure 16. Energy dissipation ratio of steel/aluminum at three impact velocities

Averaged energy dissipation ratio as a function of frequency for three different velocities for a hand-tight steel/aluminum threaded joint is shown in Fig. 16. Most noticeably, the energy dissipation ratio peak at 3.5 kHz increases with increasing impact velocity.

Energy dissipation behavior at 17 ft-lbs torque is shown in Fig. 17 at three different impact velocities. The behavior at the lowest velocity of 1.7 m/s has the most variability at frequencies below 5 kHz while a common peak is observed for all experiments at 6 kHz. The energy dissipation ratio varied from -0.18 to 0.02 at frequencies below about 1 kHz. The reason for this difference is unknown yet. The variability in torque could be a factor in the observed energy dissipation ratio below 1 kHz. The significance of a negative energy dissipation ratio (or "energy gain") will be discussed in a later section. The energy dissipation behavior at 3.7 m/s impact speed (Fig. 17b) is more consistent compared to the behavior at 1.7 m/s. The energy dissipation ratio below 1 kHz ranged from -0.2 to -0.08, but a common peak at about 5.5 kHz was observed. At the highest velocity of 6 m/s, the dissipation behavior is uniform with a maximum energy dissipation ratio of approximately 0.25 at 4.5 kHz.

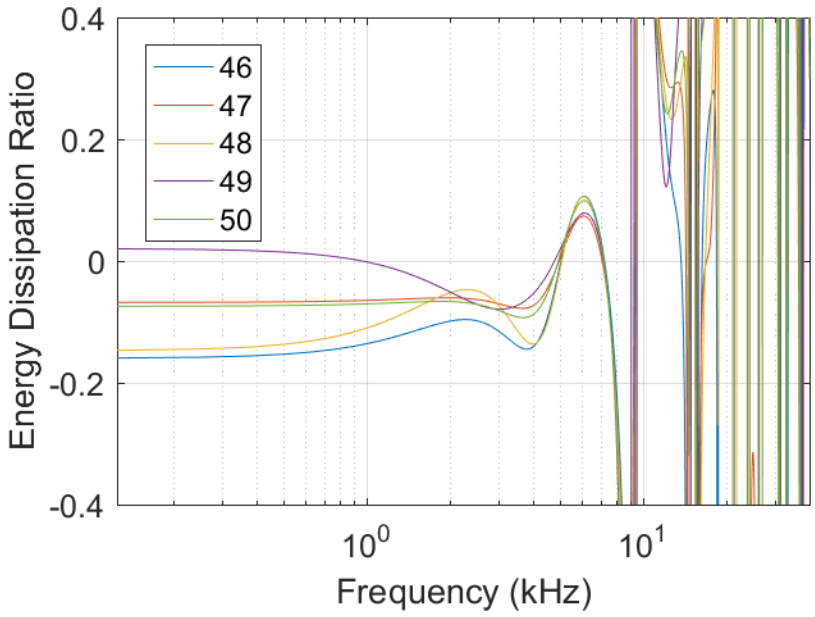

(a)

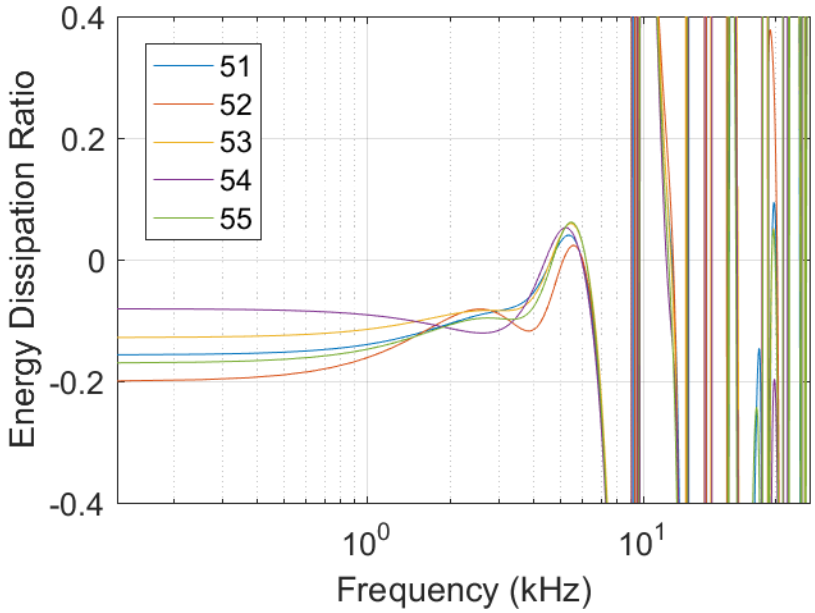

(b)

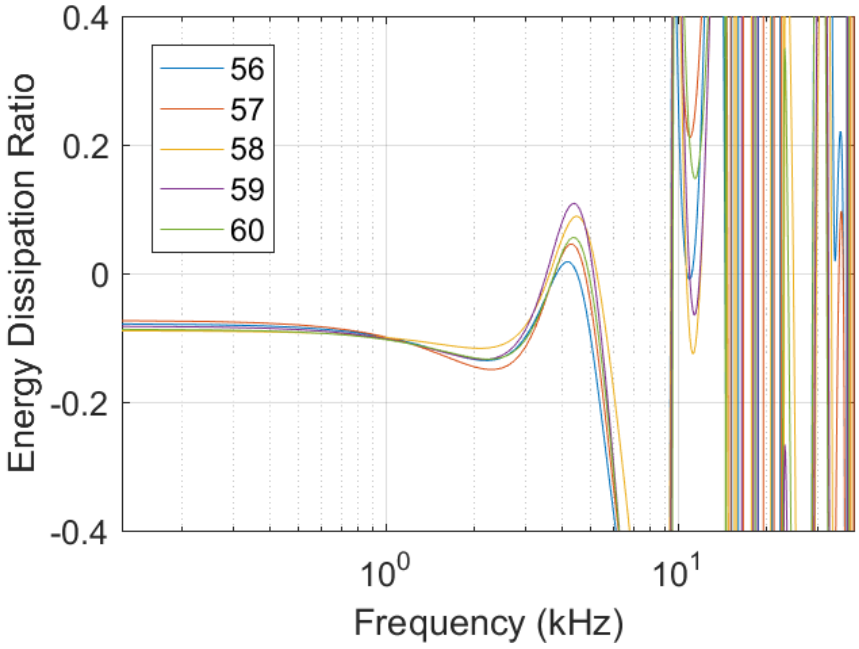

(c)

Figure 17. Frequency-domain energy dissipation ratios for steel/aluminum threaded joints at 17 ft-lbs torque for a) 1.7 m/s, b) 3.7 m/s, c) 6 m/s impact velocity

A comparison of the energy dissipation ratio at different impact velocities for 17 ft-lb torque steel/aluminum is shown in Fig. 18. Figure 18 shows that the peak energy dissipation occurred at 1.7 m/s at around 7 kHz and decreased to 5 kHz at 3.7 m/s followed by a further decrease to 4 kHz at the highest impact velocity of 6 m/s.

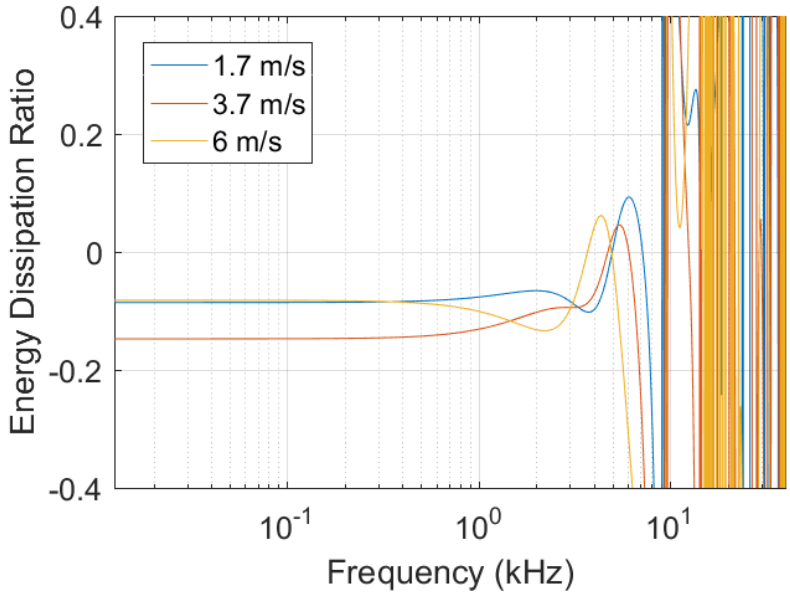

Figure 18. Effect of velocity on the energy dissipation ratio for a steel/aluminum threaded joint at 17 ft-lb torque

4.1.2. Steel/Steel Threaded Joint

The time-domain incident, reflected, and transmitted pulses from experiments at hand tight torque for steel/steel threaded joints are shown in Fig 19. Figure 19 shows that good repeatability was achieved in the time domain for each of the signals. Experiments at higher pre-torque and other impact velocities had similarly good repeatability.

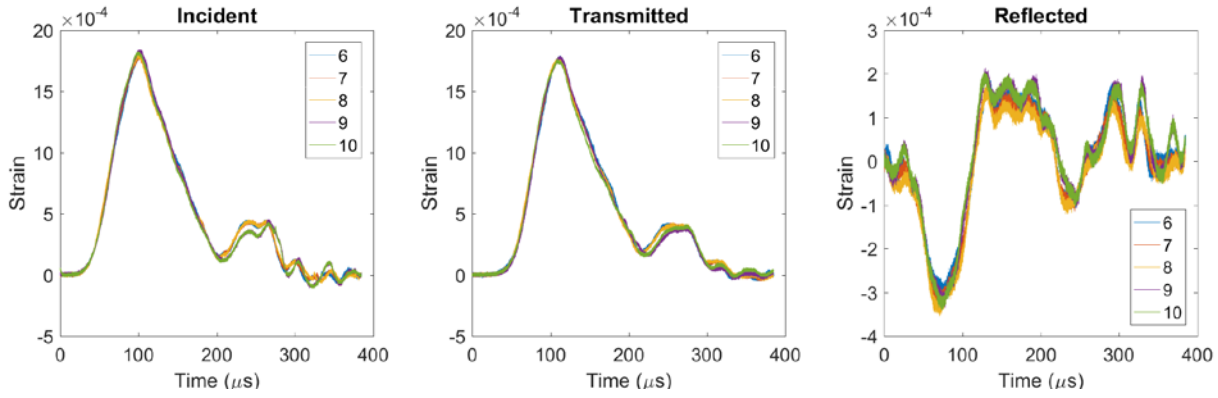

Figure 19. Time domain incident, reflected, and transmitted pulses for steel/steel threaded joints at hand tight torque for 9.6 m/s impact velocity

While the time-domain behavior of the steel/steel threaded joint was repeatable, the frequency domain behavior showed some difference. The frequency-domain energy dissipation ratios for each experiment under hand-tight torque for steel/steel threaded joints is shown in Fig. 20. While the results were repeatable at low frequencies for the 4 m/s impact velocity (Fig. 20(a)), there was variation in the frequency peak at approximately 7 kHz. At the intermediate velocity of 9.6 m/s, more variation was seen. The energy dissipation ratio at low frequencies was mostly negative for four of the experiments while for one experiment (experiment #9) the energy dissipation ratio was positive at low frequencies. Similarly, experiment #10 had higher dissipation at frequencies above 1 kHz compared to other experiments at the same velocity. When the impact velocity was increased to 13.5 m/s, the first experiment of the set (experiment #11) had a negative energy dissipation ratio across nearly the entire frequency range, but in subsequent experiments, the energy dissipation ratio cutoff frequency increased from approximately 7 kHz to over 9 kHz on the final experiment in the set. This indicates that the threaded joint dissipates energy differently with subsequent loadings compared to the first loading.

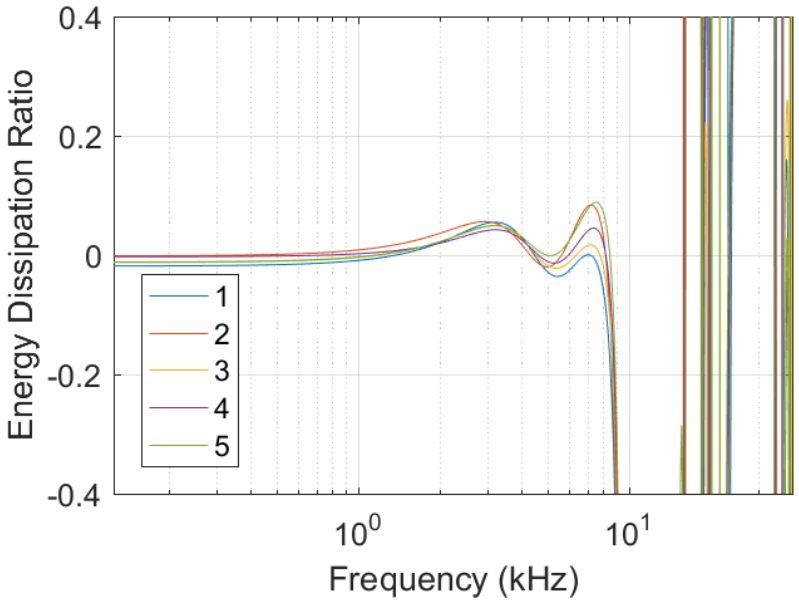
Energy Dissipation Ratio
0.4
0.2
0
-0.2
-0.4
1
2
3
4
5
10^0
10^1
Frequency (kHz)

(a)

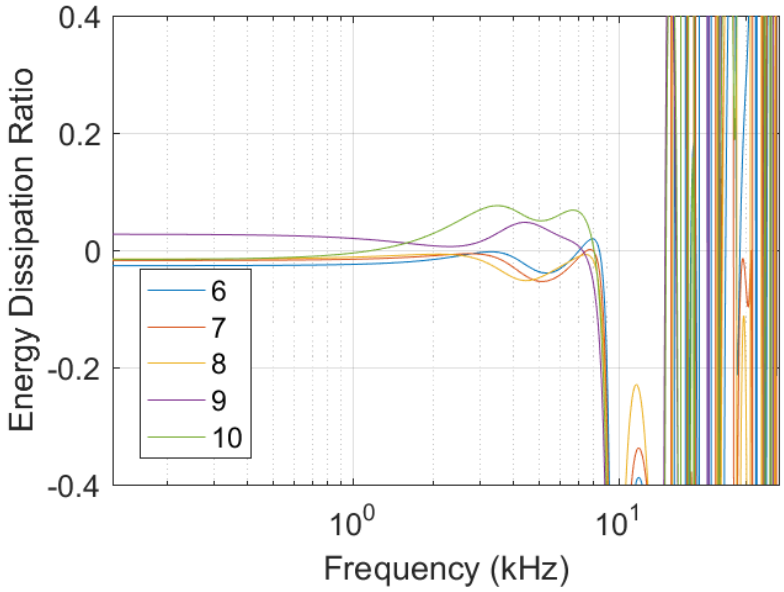
Energy Dissipation Ratio
0.4
0.2
0
-0.2
-0.4
6
7
8
9
10
10^0
10^1
Frequency (kHz)

(b)

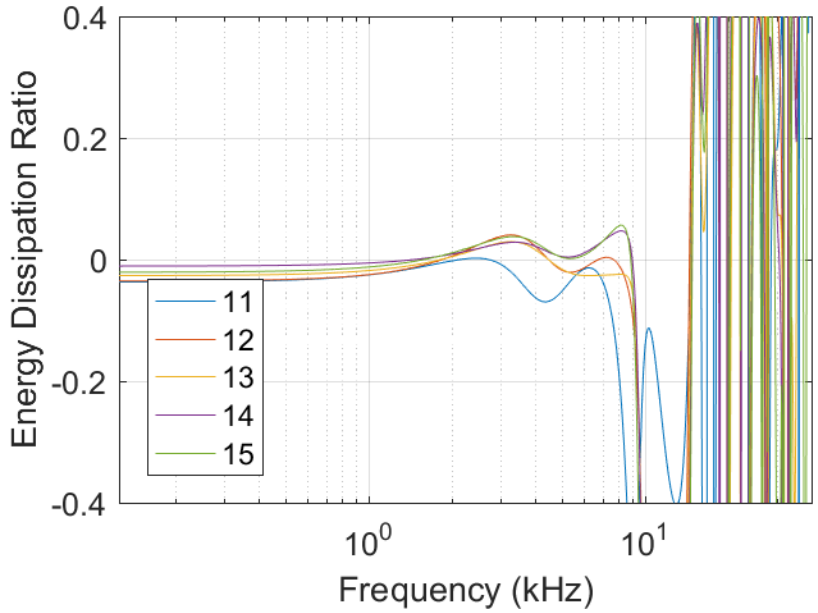

(c)

Figure 20. Frequency-domain energy dissipation ratios for steel/steel threaded joints for a) 4 m/s, b) 9.6 m/s, c) 13.5 m/s impact velocity

Figure 21 shows a comparison of the energy dissipation behavior of typical hand-tight steel/steel threaded joint at three different velocities. No clear trend in energy dissipation behavior as a function of velocity is apparent; the behavior at 4 and 13.5 m/s nearly overlaps. However, a double-peak phenomenon of energy dissipation ratio is observed at ~3 and 7 kHz, regardless of impact velocity.

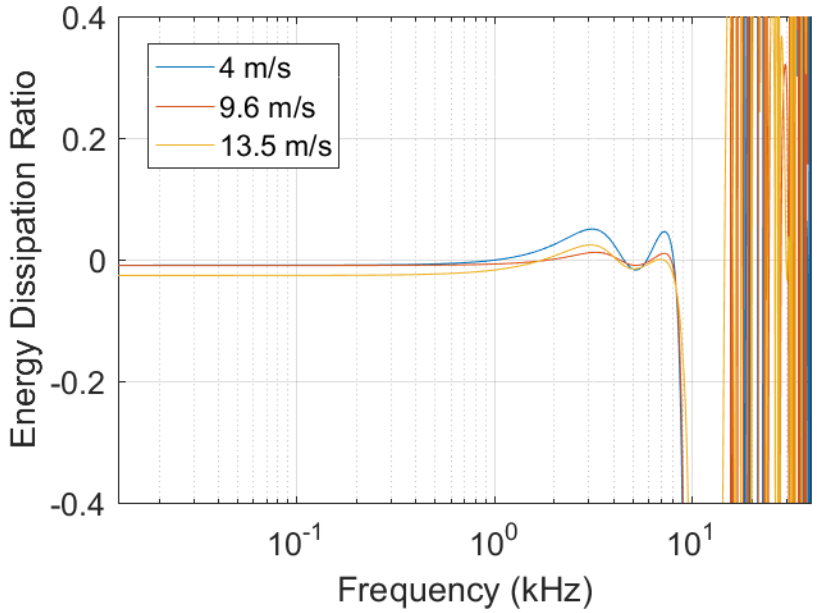

Figure 21. Steel/steel threaded joint behavior at hand-tight torque at three different impact velocities

When the steel/steel joint was torqued to 50 ft-lbs, the energy dissipation ratio behavior of the threaded joint was different. Figure 22 shows energy dissipation ratio behavior for each experiment at three different velocities. Figure 22(a) shows some indication that the threaded joint transferred/dissipated energy differently on the first experiment (experiment #16) at the lowest velocity compared to subsequent experiments. Experiment #17 at 50 ft-lbs torque and 4 m/s impact velocity had a higher peak than the rest of the experiments over 0.2 energy dissipation ratio at 6 kHz compared to the last three experiments in the set (#18, #19, #20) which indicates that a stabilized peak energy dissipation ratio is reached at a value of 0.1 energy dissipation ratio at a frequency of 6 kHz. Similarly, at the intermediate velocity of 9.6 m/s, the first experiment at that torque and impact speed (experiment #21) had a minimum energy dissipation ratio at around 3 kHz which increased by approximately 0.1 dissipation ratio in the four subsequent experiments. Likewise, at 13.5 m/s impact speed, experiment #26 had a higher energy dissipation ratio at lower frequencies compared to the final four experiments at that impact speed. Given the fact that the bars remain elastic for all experiments, the fact that the joint dissipates energy differently with successive experiments under the same torque and impact conditions is interesting. The highest stress applied to the ½" diameter thread was approximately 1.86 GPa, which occurred at the highest impact velocity. The yield stress of the C300 maraging steel at 1000 s^{-1} strain rate is approximately 2.5 GPa. This means that the steel joint was loaded to approximately 75% of yield stress, which indicates that no plastic deformation was occurring. The way the threaded joint transmits or dissipates energy under these purely elastic loading conditions must be some other mechanism than global plastic deformation. For example, over the successive dynamic experiments, the thread contact may change which may change the frequency response of impact energy dissipation.

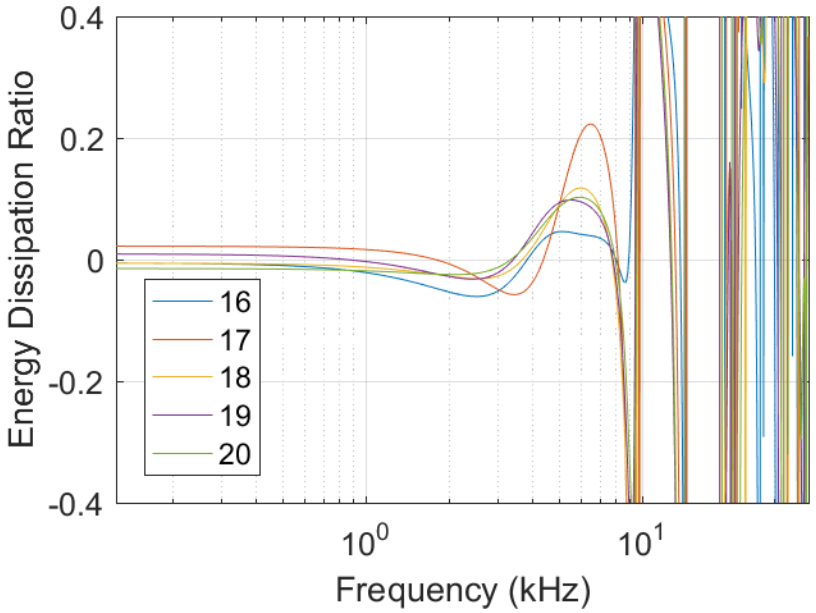
0.4
0.2
0
-0.2
-0.4
Energy Dissipation Ratio
16
17
18
19
20
10^0
10^1
Frequency (kHz)

(a)

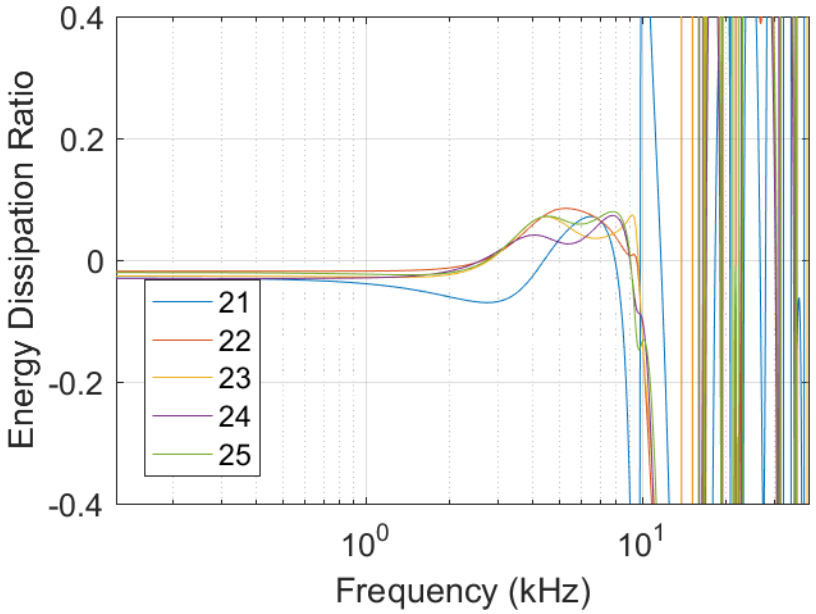
0.4
0.2
0
-0.2
-0.4
Energy Dissipation Ratio
21
22
23
24
25
10^0
10^1
Frequency (kHz)

(b)

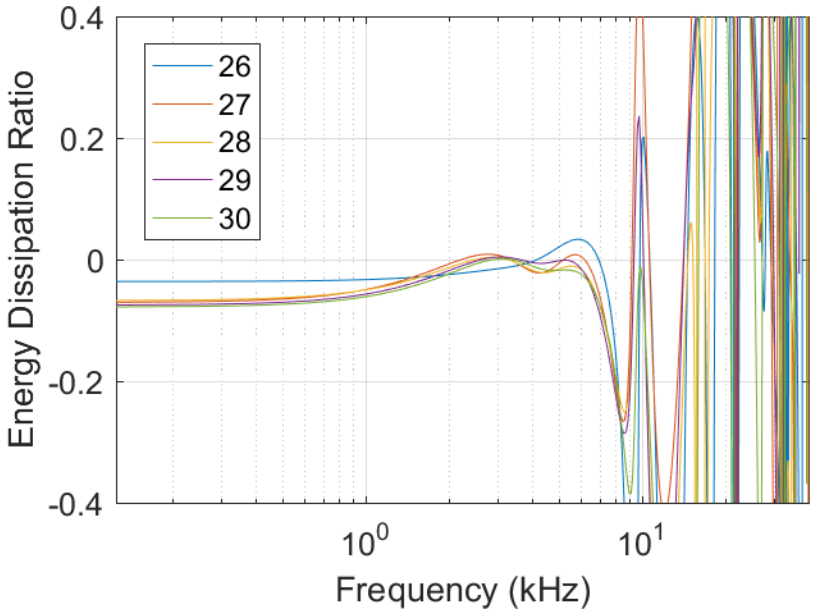

(c)

Figure 22. Energy dissipation behavior of steel/steel threaded joint torqued to 50 ft-lbs at a) 4 m/s, b) 9.6 m/s, c) 13.5 m/s impact velocity

The energy dissipation ratio of the steel/steel joint with 50 ft-lb torque shows more evidence of a relationship between impact velocity and energy dissipation behavior than that under hand-tight torque. Figure 23 shows typical energy dissipation ratio curves as a function of frequency for the three impact speeds all with 50 ft-lbs on the threaded joint. A noticeable peak of approximately 0.11 dissipation ratio at 6 kHz is evident at 4 m/s impact speed, which shrinks to approximately 0.07 dissipation peaking at about 4 kHz at 9.6 m/s, followed by another decrease to zero dissipation at 2 kHz at 13.5 m/s. The energy dissipation ratio at low frequencies also decreases with increasing impact speed; at 4 m/s the energy dissipation ratio is around zero while at 13.5 m/s the dissipation ratio is approximately 0.05 at frequencies below 1 kHz.

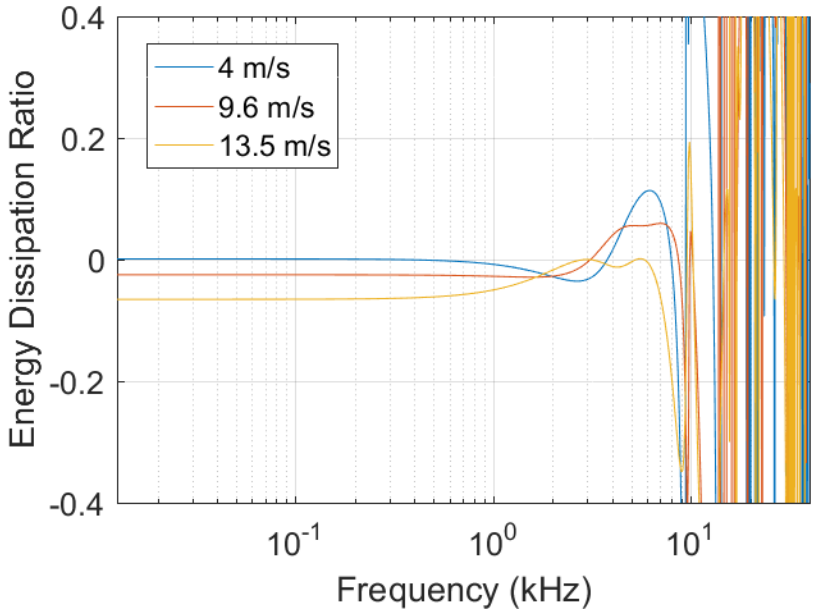

Figure 23. Energy dissipation ratio of a steel/steel threaded joint loaded at different impact velocities under 50 ft-lb torque

Comparing the effect of pre-torque at a single impact speed is useful to determine the effect of pre-torque on the frequency domain energy dissipation behavior. Figure 24 shows the energy dissipation ratios of experiments under hand-tight torque and 50 ft-lbs (which were also shown in Fig. 20(a) and Fig. 22(a)). Figure 24 however has boxes added to different frequency ranges to highlight a possible frequency shift in the energy dissipation ratio when the torque was increased. As is shown in Fig. 24, the joint with a lower pre-torque (hand-tight torque) (Fig. 24(a)) had two peaks of energy dissipation ratio, which locate in the frequency ranges of 1-5 kHz and 5-10 kHz. However, when the pre-torque was increased to 50 ft-lbs, the energy dissipation ratio peak in the frequency range of 5-10 kHz increases; whereas, the energy dissipation ratio peak in the frequency range of 1-5 kHz becomes a valley with a negative value (energy gain), as shown in Fig. 24(b). This suggests that the joint subjected to higher pre-torque dissipated more energy at 5-10 kHz compared to the same joint under hand-torque. The dissipated energy at 5-10 kHz might have been partially transferred/shifted to the low frequencies (1-5 kHz), resulting to an energy gain in the 1-5 kHz frequency range. The mechanism of such a possible frequency shift of energy dissipation is still unknown and warrants further investigation.

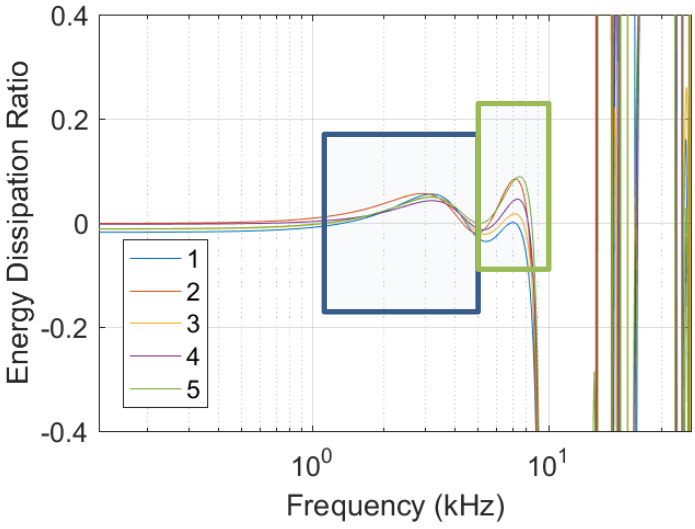

(a)

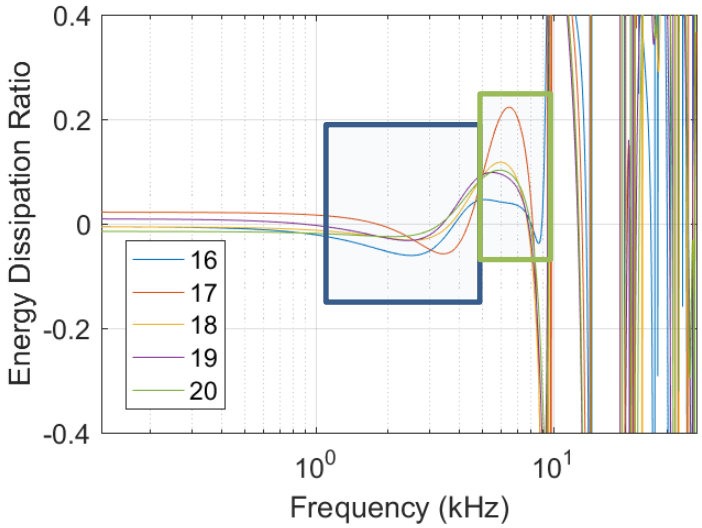

(b)

Figure 24. Possible evidence of frequency shift in steel/steel experiment on a) hand-torque compared to b) 50 ft-lb torque

4.2 Observation of Energy Gain in Threaded Joint Experiments

As shown in the previous section, many experiments had a "negative" energy dissipation ratio at low frequencies. In this section, the significance and possible cause of "energy gain" is discussed.

Energy dissipation ratio summed over the entire frequency domain, or the total energy dissipation ratio over the entire dynamic test, for steel/steel threaded joints is shown in Fig. 25. Overall, the trends in the energy dissipation behavior are difficult to discern. For hand-tight torque, initial energy dissipation at all velocities were negative. For higher velocities, the energy dissipation ratio was negative for the first three experiments in each set and positive for the last two in the set. When the torque was increased to 50 ft-lbs, all energy dissipation ratios for the first experiment in each set were negative while for the lowest velocity of 4 m/s, the remaining four experiments had positive energy dissipation. This contrasts with the all 13.5 m/s impact velocity experiments where negative energy dissipation was recorded. In general, when the impact velocity is low, i.e., 4 m/s, the steel/steel threaded joints dissipated impact energy; whereas, at higher impact velocity, i.e., 13.5 m/s, an energy gain was observed. The impact velocity where the energy dissipation transits from positive to negative seems to occur at approximately 9.6 m/s.

Energy dissipation ratios for steel/aluminum joints are shown in Fig. 26. Similar to steel/steel threaded joints, the steel/aluminum joints had tightly grouped and negative energy dissipation ratios for the first experiment in each set. All energy dissipation ratios for the steel/aluminum threaded joints were observed to be negative regardless of impact velocity and pre-torque level.

In general, energy dissipation is expected as a result of the stress wave being transmitted rather than the energy accumulation or "energy gain" that was detailed in the previous section. In an effort to understand the origin of the addition of energy into the threaded joint, the presence of the pre-torque was investigated for the possibility to cause the overall energy gain after the dynamic test is fully completed. As discussed in the previous sections, the threaded joint absorbs impact energy during loading and then release, partially or fully, the energy back to the bar system during unloading. After unloading starts, the threaded joint may be subjected to recoil to generate a release (compression) wave that propagates into the bar system. When this occurs, a compression pulse may be generated at the thread interface that could overlap with the original reflected and transmitted strain signals. Since all experiments on steel/steel threaded joints under 50 ft-lb torque at 13.5 m/s impact velocity had negative energy dissipation, the energy loss in the time domain provides a useful consideration how energy loss changed throughout the loading. The energy loss as a function of time for steel/steel threaded joint under 50 ft-lbs of pre-torque at 13.5 m/s impact speed is shown in Fig. 27. As shown in Fig. 27, the energy loss increased up until about 100 μs during the loading portion of the experiment while during the unloading portion of the experiment, the energy loss (or dissipation) becomes negative.

It is noted that the pre-torque may generate significant end to end recoil of the threaded joint. Removing the pre-torque, i.e., zero pre-torque, may reduce the end to end recoil but still general the recoil between the threads. Therefore, energy gain may still have been observed (Fig. 28) in the threaded joint experiments where a 200−μm gap was preset between the interface between the incident and transmission bars to eliminate any pre-torque. The phenomenon and mechanism of the energy gain observed in the threaded joint experiments are still unknown and warrant more systematical experimental and analytical investigation in the future.

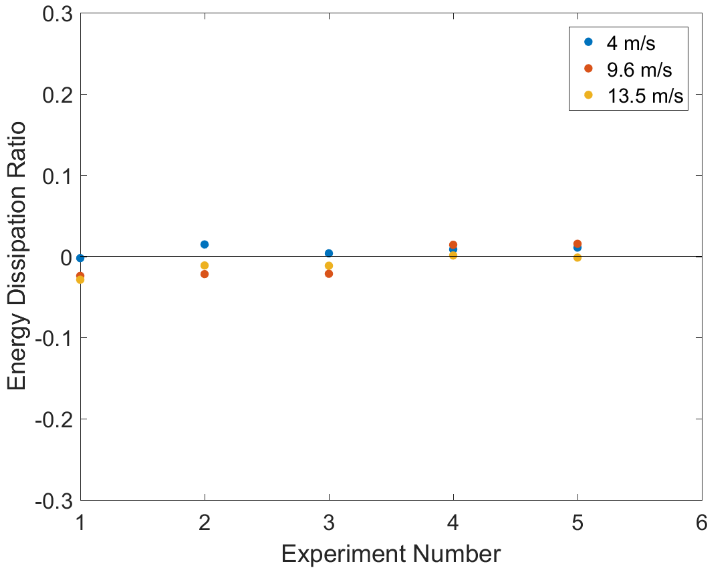

(a)

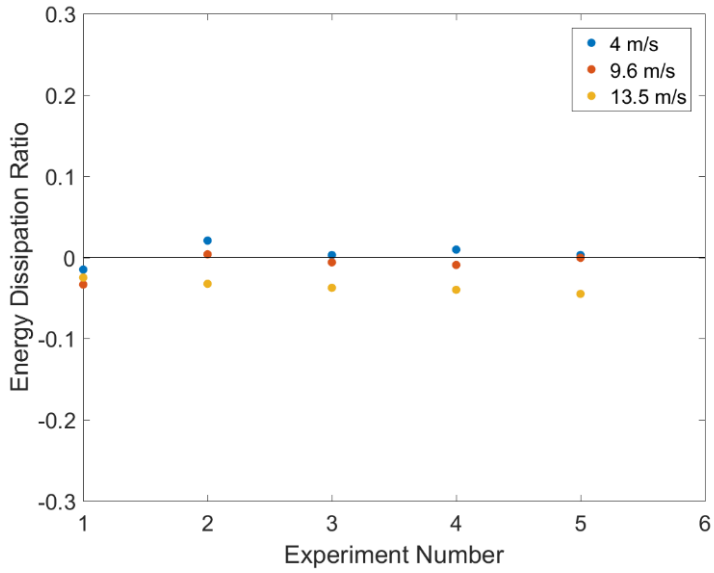

(b)

Figure 25. Energy dissipation ratio over entire frequency domain for steel/steel threaded joints under a) hand-tight torque, b) 50 ft-lb torque. "Experiment number" refers to the number of successive experiments in each set

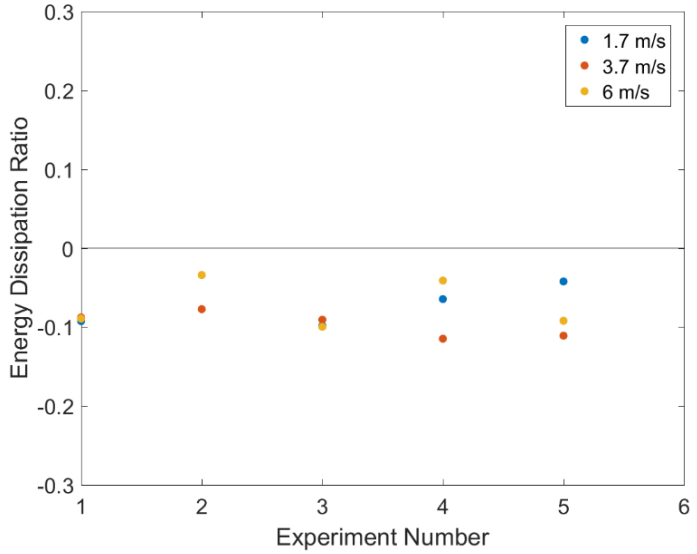

(a)

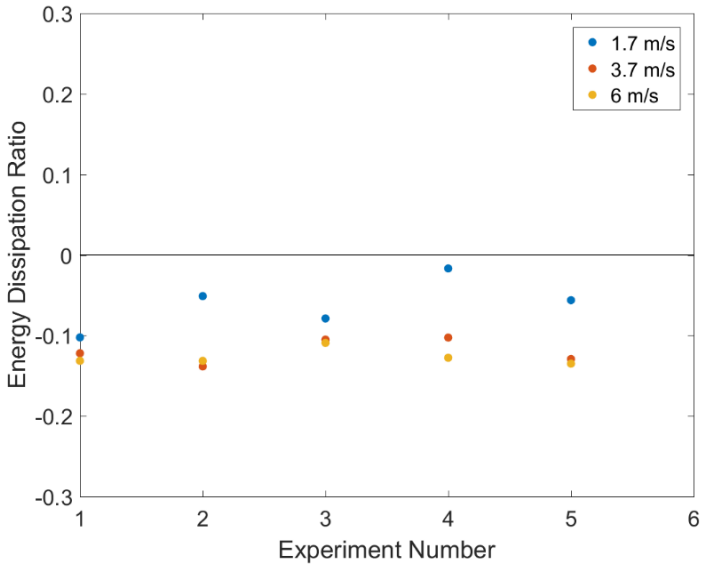

(b)

Figure 26. Energy dissipation ratio over entire frequency domain for steel/aluminum threaded joints under a) hand-tight torque, b) 17 ft-lb torque. "Experiment number" refers to the number of successive experiments in each set.

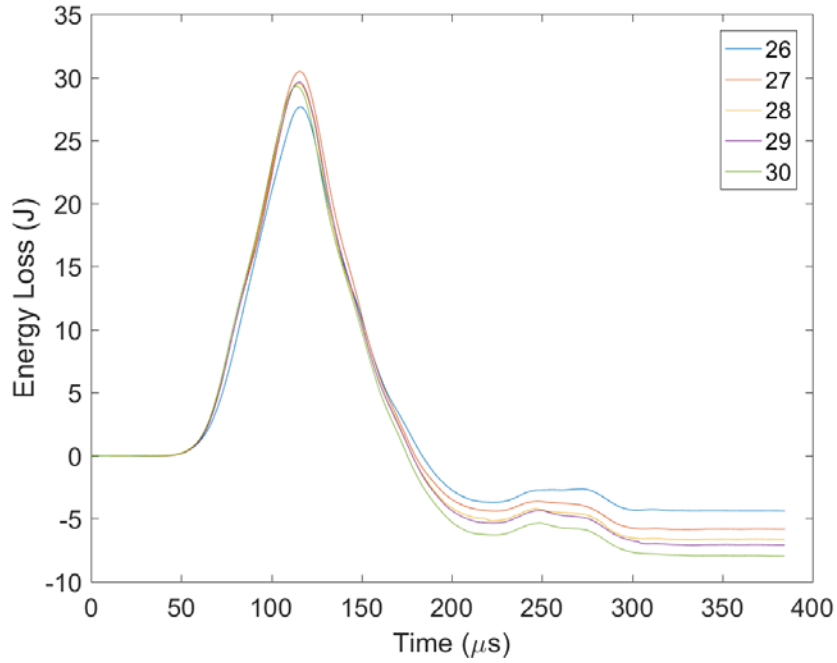

Figure 27. Energy loss for steel/steel threaded joint in the time domain for 50 ft-lb, 13.5 m/s impact velocity

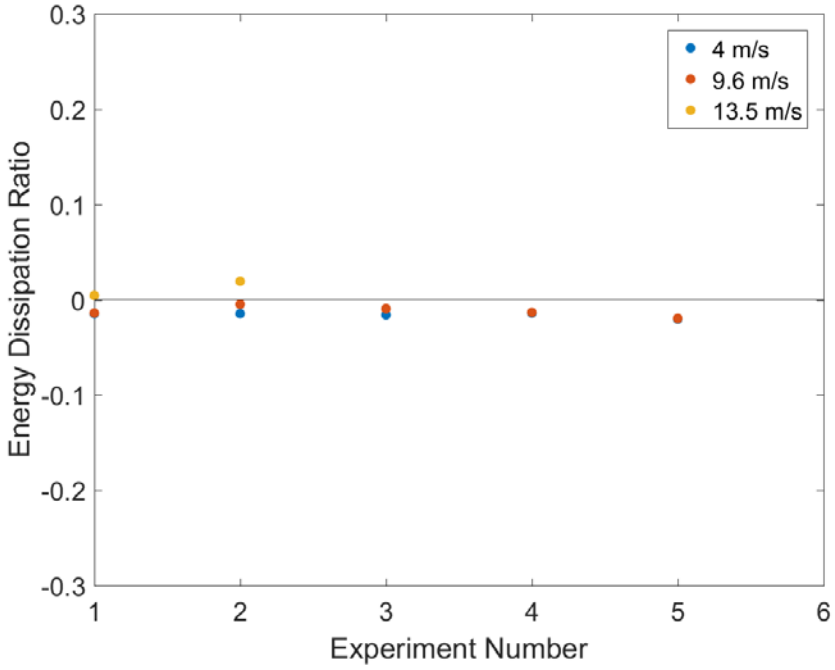

Figure 28. Energy dissipation ratio on steel/steel experiments using a gap of 200 µm between incident and transmission bars

5. CONCLUSION

Energy dissipation on threaded joints was evaluated using a Kolsky tension bar system in both time and frequency domains. To ensure that the impact energy was transferred solely across the threaded joint, a transmission bar with male threads was threaded into a female threaded incident bar. Experiments were conducted on steel/aluminum and steel/steel threaded joints. Energy dissipation behavior as a function of frequency was presented for the different joints under three impact speeds as well as two pre-torque levels. The effects of pre-torque and impact speed in the frequency domain were explored. “Negative energy dissipation” or “energy gain” was noted for different joints and impact conditions. The cause of this energy gain is still unknown, which requires further experiments and analysis in the future. The new experimental and analytical technique developed in this study can be used to investigate time- and frequency-domain energy dissipation behavior of threaded joints or any other kind of interface, which helps design and optimization of joints and interfaces. Future studies should employ the presented analysis technique, but improvements can be made to method by which threaded specimens are used. One possible method is to design a test fixture that allows the use of a new threaded joint specimen for each experiment. Using a new specimen for each experiment would also avoid potential fatigue in the threaded joint which is subjected to multiple loadings in the current configuration. This also has the potential to allow any number of threaded joint length or diameter combinations to be used, thus expanding the technique.

6. REFERENCES

1. Beccu, R. and Lundberg, B., *Transmission and dissipation of stress wave energy at a percussive drill rod joint*, International Journal of Impact Engineering 6:157-173 (1987).
2. Somasundaram, D. *Analysis of Bolted Joints Under Medium High Impact Loading*. PhD Dissertation, 2014.
3. Song, B., Antoun, B. R., Connelly, K., Korellis, J., Lu, W.-Y., *Improved Kolsky Tension Bar for High-rate Tensile Characterization of Materials*. Measurement Science and Technology, 22:045704 (7pp).
4. Chen, W., Song, B., *Split Hopkinson (Kolsky) Bar, Design, Testing and Applications,* Springer New-York, (2011).
5. Lok, T.S., Zhao, P.J., Lu, G., *Using the split Hopkinson pressure bar to investigate the dynamic behavior of SFRC.* Magazine of Concrete Research. 55, 183-191 (2003).
6. Song, B., Chen, W. *Loading and unloading splot Hopkinson pressure bar pulse-shaping techniques for dynamic hysteretic loops*. Experimental Mechanics. 44, 622-627 (2004).
7. Thompson, B., Pramod, N., Smith, D., *Reducing bolt preload variation with angle-of-twist bolt loading*. AIAA Joint Propulsion Conference, Salt Lake City, Utah (2001)
8. National Air and Space Administration. *Space Shuttle: Criteria for Preloaded Bolts*. NSTS 09307. (1998)

DISTRIBUTION

1 OUSD(AT&L)/(A)/TWS-LW&M
Attn: Chris Cross
3090 Defense Pentagon, Room 3B948A
Washington, DC 20301

1 Air Force Office of Scientific Research/RTA
Attn: Martin Schmidt
875 N. Randolph St.
Arlington, VA 22203-1768

1 Naval Air Warfare Center Weapons Division (NAWCWD)
Attn: J Grover
2400 East Pilot Plant Road Stop 5402
Building 11091 Room 1
China Lake CA, 93555

1 U.S. Army Armament Research Development and Engineering Center
Attn: J.A. Cordes
RDAR-MEA-A
Engineering Analysis and Evaluation Division Armaments Engineering and Analysis & Manufacturing Directorate
Picatinny Arsenal, NJ 07806-5000

1	MS0557	B. Sanborn	1528
1	MS0557	B. Song	1528
1	MS0557	D.J. Kenney	1528
1	MS0557	T. Martinez	1528
1	MS0557	R. Everett	1528
1	MS0557	D. Jones	1528
1	MS0557	D. Croessmann	1520
1	MS1160	E. Nishida	5421
1	MS1160	D. Dederman	5421
1	MS1160	J. Brown	5421
1	MS1160	R. Terpsma	5421
1	MS1160	W. Maines	5414
1	MS1218	A. Brundage	5414
1	MS1164	M. Atkins	10654
1	MS0899	Technical Library	9536 (electronic copy)


Sandia National Laboratories